Mammalian mitochondrial inorganic polyphosphate (polyP) and cell signaling: Crosstalk between polyP and the activity of AMPK

Renata T da Costa, Anna Nichenko, Matheus M Perez, Malgorzata Tokarska-Schlattner, Sheida Kavehmoghaddam, Vedangi Hambardikar, Ernest R Scoma, Erin L Seifert, Uwe Schlattner, Joshua C Drake, et al.

Original article

MOLECULAR METABOLISM

Mammalian mitochondrial inorganic polyphosphate (polyP) and cell signaling: Crosstalk between polyP and the activity of AMPK

Renata T. Da Costa[1], Anna Nichenko[2], Matheus M. Perez[1], Malgorzata Tokarska-Schlattner[3], Sheida Kavehmoghaddam[1], Vedangi Hambardikar[1], Ernest R. Scoma[1], Erin L. Seifert[4], Uwe Schlattner[3], Joshua C. Drake[2], Maria E. Solesio[1,*]

ABSTRACT

Inorganic polyphosphate (polyP) is an evolutionary and ancient polymer composed by orthophosphate units linked by phosphoanhydride bonds. In mammalian cells, polyP shows a high localization in mammalian mitochondria, and its regulatory role in various aspects of bioenergetics has already been demonstrated, via molecular mechanism(s) yet to be fully elucidated. In recent years, a role for polyP in signal transduction, from brain physiology to the bloodstream, has also emerged.

Objective: In this manuscript, we explored the intriguing possibility that the effects of polyP on signal transduction could be mechanistically linked to those exerted on bioenergetics.

Methods: To conduct our studies, we used a combination of cellular and animal models.

Results: Our findings demonstrate for the first time the intimate crosstalk between the levels of polyP and the activation status of the AMPK signaling pathway, via a mechanism involving free phosphate homeostasis. AMPK is a key player in mammalian cell signaling, and a crucial regulator of cellular and mitochondrial homeostasis. Our results show that the depletion of mitochondrial polyP in mammalian cells downregulates the activity of AMPK. Moreover, increased levels of polyP activate AMPK. Accordingly, the genetic downregulation of AMPKF0611 impairs polyP levels in both SH-SY5Y cells and in the brains of female mice.

Conclusions: This manuscript sheds new light on the regulation of AMPK and positions polyP as a potent regulator of mammalian cell physiology beyond mere bioenergetics, paving the road for using its metabolism as an innovative pharmacological target in pathologies characterized by dysregulated bioenergetics.

Keywords Inorganic polyphosphate; Mitochondria; Mammalian cells; Cell signaling; AMPK; Bioenergetics

1. INTRODUCTION

Inorganic polyphosphate (polyP) is an ancient and well-conserved throughout evolution polymer. PolyP consists of chains of orthophosphate units linked by phosphoanhydride bonds, which are structurally similar to the bonds that link phosphates in ATP [1–3]. PolyP is involved in the regulation of a plethora of cellular processes, ranging from biofilm formation, to collagen folding [4–6]; and it is one of the diverse structural forms in which inorganic phosphate (Pi) is found in living organisms. Accordingly, its role in the storage of mobilizable Pi has already been demonstrated in simple organisms [3]. Pi is commonly described as a major backbone of life, due to its essential role in the regulation of many biochemical pathways, including energy metabolism and cellular signaling [7–9].

Mammalian polyP exhibits high mitochondrial levels [10–15] (even though high levels of the polymer have also been described in other mammalian sub-cellular compartments, such as the acidocalcisomes, and the nucleolus [16–19]), and previous studies by us and others have already demonstrated its regulatory role in different aspects of mitochondrial bioenergetics [2,13,14,20–29]. Moreover, polyP is involved in the regulation of other mammalian processes that are highly energy-dependent and closely related to mitochondrial function, such as the maintenance of proper protein homeostasis; including the regulation of amyloidogenesis [30–32], and proteostasis within the organelle [33]. While the relationship between the levels of polyP and the status of mammalian bioenergetics is becoming increasingly clear; the molecular mechanisms by which polyP exerts its regulatory effects on energy metabolism remain poorly understood. One plausible mechanism which

[1]Department of Biology, and Center for Computational and Integrative Biology, Rutgers University, Camden, NJ, USA [2]Department of Human Nutrition, Foods, and Exercise, Virginia Polytechnic Institute and State University, Blacksburg, VA, USA [3]University Grenoble Alpes, Inserm U1055, Laboratory of Fundamental and Applied Bioenergetics, Grenoble, France [4]MitoCare and Department of Pathology and Genomic Medicine, Thomas Jefferson University, Philadelphia, PA, USA

*Corresponding author. Rutgers University, 201 Broadway, Camden, NJ, 08103, USA. Tel.: +1856 225 6395. E-mail: m.solesio@rutgers.edu (M.E. Solesio).

Received October 14, 2024 • Revision received November 22, 2024 • Accepted November 26, 2024 • Available online 30 November 2024

https://doi.org/10.1016/j.molmet.2024.102077

garnered attention in the past few years involves the role of polyP on cellular signaling transduction, affecting processes that range from mammalian brain physiology [34,35], to blood circulation [36–38].

Intracellular signaling is a potent mechanism for regulating mitochondrial function [39], with the adenosine monophosphate (AMP)-activated protein kinase (AMPK), a serine/threonine kinase which has been well-conserved throughout evolution [40,41], representing a major signaling hub in the organelle [40,42]. The activation of AMPK is a highly complex process, but the major role played by decreased ATP:ADP and ATP:AMP ratios on promoting phosphorylation at its Thr172 site, while inhibiting dephosphorylation, has already been demonstrated [43–45]. Mitochondria not only regulate AMPK by their functional state via its energy sensing capacity, but vice versa; AMPK can also modulate mitochondrial function via downstream targets [46]. Interestingly, inositol polyP, another complex form of Pi, has already demonstrated critical regulatory effects on AMPK activity [47,48]. Moreover, recent studies have shown the presence of AMPK in the outer mitochondrial membrane [49,50] (in addition to its known cytoplasmic and nuclear locations [51]), where it may sense dysfunctional oxidative ATP synthesis, even prior to the disruption of the mitochondrial membrane potential [52]. AMPK activation also increases glucose uptake and glycolytic flux [53,54], and can therefore participate in a switch from oxidative to glycolytic metabolism. Indeed, decreased ATP:ADP ratios and increased glycolysis are hallmarks of various human pathologies [55–57], and are also found in mammalian cells depleted of mitochondrial polyP [26,29].

The metabolism of polyP is well-described in prokaryotes and simple eukaryotes. In fact, the role of endopolyphosphatases (PPN, which mediate the non-processive cleavage of polyP), exopolyphosphatases (PPX, which cleavage polyP at the terminal Pi), and polyP kinases (PPK) is well-known, as well as it is the regulatory role of these enzymes in the intracellular levels of Pi [6,58–65]. Despite recent research efforts, the identification of mammalian homologs of PPN, PPX, and PPK remains elusive [66–68]. By the expression of the PPX enzyme in mammalian mitochondria, we have created MitoPPX cells. We have already fully characterized these cells, including addressing the status of bioenergetics, cell viability, calcium homeostasis, etc. [14,25,26,28,29,33,69,70]. In these previous works, significantly decreased levels of polyP, and dysregulated bioenergetics were always described in MitoPPX cells, when compared to the control samples.

As mentioned above, the regulatory role of mammalian polyP in various aspects of bioenergetics is known. However, the molecular mechanism(s) underlying this effect still remains mostly unknown. Here, using Wild-type (Wt) and MitoPPX SH-SY5Y cells, our findings corroborate the profound effects that the depletion of mitochondrial polyP has in mammalian bioenergetics. Moreover, we show a new, intimate crosstalk between polyP levels and the activation status of AMPK, which could be mediated by a mechanism involving free Pi homeostasis. These findings may at least partially explain the effects of the polymer on bioenergetics. Our results also suggest the metabolism of polyP as a valid and innovative pharmacological target in human diseases where dysregulated bioenergetics is present.

2. MATERIALS AND METHODS

2.1. Reagents

Dulbecco's Modified Eagle medium (DMEM)/F12, penicillin/streptomycin, geneticin, heat-inactivated fetal bovine serum (FBS), and trypsin were acquired from Gibco-Invitrogen (Carlsbad, California, USA). Phosphate-buffered saline (PBS), dimethyl sulfoxide (DMSO), ethanol, D-glucose monohydrate, glycerol, Triton X-100, phenylmethylsulfonyl fluoride (PMSF), potassium chloride (KCl), tris(hydroxymethyl)-1,3-propanediol hydrochloride (TRIS—HCl), sucrose, mannitol, magnesium chloride ($MgCl_2$), ethylenediaminetetraacetic acid (EDTA), ethylene glycol-bis(2-aminoethylether)-N,N,N′,N′-tetraacetic acid (EGTA), β-mercaptoethanol, methanol, tween-20, perchloric acid, potassium carbonate (K_2CO_3), trizma base, 1,4-dithiothreitol (DTT), sodium azide, lactobionic acid, taurine, [4-(2-hydroxyethyl)-1-piperazineethanesulfonic acid] (HEPES), bovine serum albumin fatty acid-free (BSA), potassium phosphate monobasic (KH_2PO_4), imidazole, oligomycin, antimycin A, sodium phosphate monobasic, and carbonyl cyanide m-chlorophenyl hydrazone (CCCP) were acquired from Sigma—Aldrich (St. Louis, Missouri, USA). 4′,6-diamidino-2-Phenylindole (DAPI), lipofectamine, RIPA lysis buffer, Pierce BCA protein assay kit, Pierce ECL western blotting substrate, Pierce halt protease inhibitor, Opti-minimal essential medium (MEM), TRIzol, and proteinase K were acquired from ThermoFisher Scientific (Waltham, Massachusetts, USA). Dnase I and Rnase A from the bovine pancreas, as well as phosSTOP phosphatase inhibitors, were acquired from Millipore Sigma (Burlington, Massachusetts, USA). The serine/threonine phosphatase assay was acquired from Promega (Madison, Wisconsin, USA). Power SYBR™ Green PCR Master Mix was acquired from QIAGEN (Hilden, Germany). The scramble siRNA (sc-37007) and AMPKα_1 siRNA (sc-29673) were acquired from Santa Cruz Biotechnology (Dallas, Texas, USA). All reagents and materials used in immunoblots, including secondary antibodies (anti-mouse, cat. num.: 1706516; and anti-rabbit, cat. num.: 1706515), protein ladder, fat-free milk, polyvinylidene membranes (PVDF), polyacrylamide pre-cast gels, Laemmli sample buffer, Tris/Glycine/SDS buffer, and Tris/Glycine buffer were acquired from BioRad (Hercules, California, USA). Specific primary antibodies used and catalog numbers are included in the immunoblot section of these methods. The scPPX enzyme was a kind gift from Dr. James H. Morrissey's Laboratory (University of Michigan, Michigan, USA); and synthetic polyP (≅ 14 Pi units, short chain) was a kind gift from Dr. Toshikazu Shiba (Kitasato University, Tokyo, Japan).

2.2. Cell cultures

SH-SY5Y cells were purchased from the ATCC (Manassas, Virginia, USA) and maintained in culture following the instructions provided by the vendor, and our previously published protocols [71,72]. Experiments were conducted in all cases when cells were at an approximate confluence of 80%. MitoPPX cells were created, characterized, and maintained as previously described [26,70]. These cells stably express the active yeast PPX1 enzyme, targeted to mitochondria. Moreover, in some key experiments, we used a mutated expressing version of the MitoPPX construct as a control condition. Specifically, we created a plasmid with a point mutation in the asparagine 127 (^{D127N}) of the PPX1 (^{D127N}MitoPPX SH-SY5Y cells, asparagine was replaced by aspartic acid). This mutation prevents the substrate specificity of the enzyme, therefore inhibiting its activity [60]. A brief characterization of these cells is included in this manuscript.

2.3. Mitochondrial isolation

Mitochondrial-enriched fractions were obtained from SH-SY5Y cells via differential centrifugation in a mannitol/sucrose buffer, following our previously published protocols [73,74]. Lysis and protein quantification were performed on the day of the experiments. Protein content was quantified on the obtained mitochondrial-enriched lysates using the Pierce BCA assay kit, and following the instructions from the manufacturer.

2.4. High-resolution respirometry (HRR)

Mitochondrial respiration was quantified by HRR, using Oroboros-O2k (Oroboros instruments, Innsbruck, Austria) in intact cells, following the previously described protocol [68]. Briefly, 2×10^6 cells were resuspended in Mir05 buffer (110 mM D-sucrose, 20 mM HEPES, 10 mM KH_2PO_4, 20 mM taurine, 60 mM lactobionic acid, 3 mM $MgCl_2$, 0.5 mM EGTA, and 1 g/L BSA at pH 7.1); and loaded into a 2 mL chamber at 37 °C, under constant stirring. The oxygen concentration was maintained around 190 μM. Subsequently, the baseline respiration rate was recorded, and the respiratory parameters were determined after titration with 0.5 μM oligomycin A, 1 μM CCCP, and 50 nM antimycin A. Data was recorded using the DataLab Software 4 (Oroboros Instruments, Innsbruck, Austria). In all respiratory parameters, the oxygen flux rate was corrected for non-mitochondrial respiration. Data is presented as mean ± SEM from at least three biological replicates and experimental duplicates per biological replicate, and results are expressed as pmol O_2/s/10^6 cells.

2.5. Quantification of the intracellular ADP:ATP ratio

3×10^6 cells were seeded in cell culture-treated dishes. After 48 h, culture media was removed, and cells were washed twice on ice-cold 1x PBS. Cell lysis was then performed by adding 0.5 mL of ice-cold 0.6 N (3.5%) perchloric acid, and quickly scraping and centrifuging the samples for 2 min at 18,000×*g* and 4 °C. Supernatants were then neutralized for 30 min with K_2CO_3 (pH 6.5–7.5), and centrifuged again for 10 min at 18,000×*g* and 4 °C. Lastly, supernatants were recovered, flash-frozen in liquid N_2, and stored at −80 °C. Adenine nucleotides were determined in supernatants by HPLC (Varian 410, France) with an RP-C18 column (Polaris C18-A 250 × 4.6 mm, 5 μm, Varian, France) at 1 mL/min flow rate and 30 °C, as described in detail elsewhere [75]. Briefly, protein-free extract (75 mL premixed with 50 mL mobile phase) was separated in pyrophosphate buffer (28 mM, pH 5.75); detection was performed at 254 nm; ATP and ADP were eluted at 6.5 and 8 min, respectively. Elution peaks were integrated using the STAR software (Varian, France). ATP and ADP concentrations in lysates were obtained using calibration curves, and the corresponding ATP:ADP ratios were calculated. Note that under the applied experimental conditions, AMP was not detectable.

2.6. Immunoblots

Immunoblots were conducted following our previously published protocol [26,28,76]. In the case of the phospho-antibodies, samples were lysed in regular lysis buffer that also contained 1x PhosSTOP. Regarding the immunoblots performed in mice tissue, we used the right hemisphere of the brains to conduct these experiments, which were conducted following the previously published protocol [41]. The following primary antibodies were used:

2.7. Phosphatases assay

Cells were loaded into 150 cm^2-treated culture dishes at a density of 4×10^6 cells/dish, and collected 48 h later. The phosphatase assay was then conducted following the instructions provided by the manufacturer (see "reagents"). As a negative control, 1x phosphatase inhibitor (PhosSTOP) was used. Data is presented as mean ± SEM from at least three biological replicates and experimental duplicates per biological replicate.

2.8. Mitochondrial mass quantification

5×10^5 Wt and MitoPPX SH-SY5Y cells per well were seeded in 6-well plates and cultured for 48 h before harvesting. Extraction of total DNA and quantitative PCR (qPCR) was conducted following a protocol adapted from Fazzini et al., [77]. Briefly, cell pellets were resuspended in 1x RIPA lysis buffer supplemented with 1 mg/mL proteinase K. Subsequently, samples were incubated at 65 °C for 24 h; DNA was extracted using phenol-chloroform-isoamyl alcohol, and protein concentration was quantified by spectrophotometry (NanoDrop One, GE Health Care, Buckinghamshire, United Kingdom). qPCR analysis was then performed to determine the number of mitochondrial DNA (mtDNA) copies, relative to the levels of nuclear DNA (nDNA). Primers were designed following a previously published protocol (we used $tRNA^{Leu}$ for mitochondrial DNA and β-2-microglobulin -BMA-for nuclear DNA [78]). Each primer was used at a final concentration of 400 nM. The sequence of the primers is included in the Supplementary Table.

Vendor	Cat n.	Name
AbCam (Cambridge, Cambridgeshire, UK).	Ab225684	Anti-PPX
	Ab3759	Anti-AMPKα_1
	Ab3760	Anti-AMPKα_2
	Ab56889	Anti-Mfn2
Cell signaling Technology (Danvers, Massachusetts, USA).	CST-3700	Anti-β-actin
	CST-2535	Anti-^{T172}pAMPK$\alpha_{1/2}$
	CST-4185	Anti-^{S485}pAMPK$\alpha_{1/2}$
	CST-2532	Anti-AMPK$\alpha_{1/2}$
	CST-13038	Anti-^{T308}pAkt
	CST-4060	Anti-^{S473}pAkt
	CST-9272	Anti-Akt
	CST-3482	Anti-^{S428}pLKB1
	CST-2083	Anti-^{S792}pRaptor
	CST-2280	Anti-Raptor
	CST-5759	Anti-pAMPK substrate motif [LXRXX(pS/pT)]
	CST-5391	Anti-Drp1
	CST-3661	Anti-^{S79}pACC
	CST-3662	Anti-ACC$_{1/2}$
Santa Cruz Biotechnology (Dallas, Texas, USA).	Sc-32282	Anti-Parkin
	Sc-374292	Anti-IP6K1
	Sc-130012	Anti-IP6K2
Sigma—Aldrich (St. Louis, Missouri, USA).	SAB5700771	Anti-LKB1
ThermoFisher Scientific (Waltham, Massachusetts, USA).	PA5-21908	Anti-XPR1 (SLC53A1)

The qPCR was performed on a QuantStudio™ 6 Flex Real-Time PCR System (Applied Biosystems, Foster City, California, USA), using Power SYBR™ Green PCR Master Mix, and following the instructions provided by the manufacturer. Moreover, the following specific conditions were used: hot start at 95 °C for 10 min, followed by 40 cycles of 95 °C for 15 s, and 62 °C for 25 s. The $^{\Delta}$Ct was obtained by subtracting the average nDNA Ct values from the average mtDNA Ct values. The number of relative mtDNA copies was calculated by raising two to the power of the $^{\Delta}$Ct and then multiplying by two to account for the diploid nature of the nuclear genome (nDNA-mtDNA $= 2^{\Delta}\text{Ct} \times 2$). The results are shown as FC.

2.9. Treatment with exogenous polyP

2×10^6 Wt SH-SY5Y cells were seeded on treated-culture dishes and incubated for 48 h. Media was then replaced, and the experimental group was treated with 25 μM short-chain polyP ($polyP_{14}$, sodium salt, concentration is expressed in terms of Pi units) diluted in ultrapure water (stock concentration, average length ≅ 14 Pi units), while the control group was treated only with the vehicle. Both polyP and the vehicle solutions were diluted to their working concentrations in complete DMEM/F12. Cells were incubated for 24 h and subsequently

washed twice with cold 1x PBS. Cell pellets were then collected by scraping the cells on iced-cold 1x PBS, and they were dissolved in lysis buffer containing protease and phosphatase inhibitors. Supernatants were also collected for further analysis. To confirm the cellular uptake of exogenous polyP, a DAPI-polyP assay was conducted in whole cells and isolated mitochondria from $polyP_{14}$-treated cells. Immunoblots were also performed to determine the effects of increased polyP on the α-T172 phosphorylation of AMPK.

2.10. Treatment with Pi

Cells were seeded and grew similarly to those treated with exogenous polyP. In this instance, a stock solution of sodium phosphate monobasic was prepared by diluting it in ultra-pure water. Cells were treated for 24 h with the stated concentrations of Pi, obtained by diluting the stock solution in the growing medium. Control samples were treated with vehicle only. Cells were then collected, and the experiments were carried out following the same procedures as those used for the treatment with exogenous polyP.

2.11. Cytotoxicity assay

To conduct this experiment, 5×10^5 cells/well were seeded in each well of 6-well plates. The experiment was conducted following the instructions provided by the manufacturer (see "reagents"). Cells were treated with 25–500 μM of either exogenous $polyP_{14}$ or Pi. Absorbance was measured at 492 and 620 nm using a microplate reader (CLARIOstart spectrophotometer, BMG Labtech, Ortenberg, Germany). Blank values were subtracted from the obtained results, and sample values were normalized based on the LDH levels obtained on the vehicle-only samples. Data is presented as mean ± SEM from at least three biological replicates and experimental duplicates per biological replicate.

2.12. Mice

All experimental procedures were approved by the Institutional Animal Care and Use Committee (IACUC) at Virginia polytechnic Institute and State University. Mice were housed in temperature-controlled (21 °C) quarters with a 12:12 h light–dark cycle and *ad libitum* access to chow (Purina) and water. $AMPK\alpha1^{T172A}$ knock-in mice were generated using CRISPR/Cas9-mediated gene editing at Genetically Engineered Murine Model Core at the University of Virginia as described [79]. The target sequence for the guide RNA (gRNA) is 5′-GAATTTTTAAGAACAAGCTGG-3′, in which TGG is the protospacer adjacent motif (PAM) sequence and ACA is the codon for threonine 172 (^{T172}) that is mutated to GCT for alanine. Resulting mice were crossbred with C57BL/6J mice for at least seven generations before being maintained via heterozygous breeding pairs. Pups from heterozygous pairing were used for study, and sequencing of tail DNA confirmed genotype. Following an overnight fast (12 h), mice were anesthetized with 3% isoflurane and euthanized via cervical dislocation. Tissues were collected and flash-frozen in liquid N_2, prior shipment on dry ice to the Rutgers laboratory.

2.13. DAPI-polyP assay

The DAPI-polyP fluorescence assay was used to quantify mitochondrial polyP in cellular and tissue samples. DAPI-DNA complexes exhibit a maximum fluorescence at 450 nm. However, polyP specifically shifts the fluorescence emission of associated DAPI towards higher wavelengths ($\lambda_{ex} = 405$ nm). This method is broadly used by the polyP research community [16,80,81]. Some differences in the protocol were introduced depending on the nature of the samples:

2.13.1. Cellular samples

2×10^6 SH-SY5Y cells were seeded in cell culture-treated dishes, and washed and harvested on iced-cold 1x PBS when they were approximately at an 80% confluency. Subsequently, the cell suspension was centrifuged for 5 min at 250×*g* and 4 °C; and mitochondria were isolated as previously described. The mitochondrial-enriched pellet was lysed with a buffer containing 30 mM Tris–HCl, pH 7.4, 200 mM KCl, 0.5% Triton, 1x protease inhibitor cocktail, and 1 mM PMSF for 10 min on ice, following the protocol previously published [70]; and protein content was quantified using the Pierce BCA protein assay kit, and following the protocol provided by the manufacturer. 50 μL of cell lysates were loaded into a well of a 96-well black half-area plate at a protein concentration of 0.1 μg/μL. A standard curve with synthetic polyP (0, 0.5, 2, 5, 7, and 15 μM) was also prepared using sodium $polyP_{14}$. PolyP standards and samples were diluted in a buffer containing 75 mM sucrose, 225 mM mannitol, and 5 mM Tris–HCl pH 7.4. DAPI was added to each well at a final concentration of 10 μM. Samples and standards were assayed in experimental and biological triplicates. PolyP levels obtained in the experimental conditions were standardized to those obtained in the Wt cells. Data is presented as mean ± SEM from at least three biological replicates and experimental triplicates per biological replicate.

2.13.2. Brain tissue analysis

The left hemisphere of mice brains was used for the DAPI-polyP analysis. Brains were weighed and homogenized using the tissue homogenization buffer (30 mM Tris–HCl, pH 7.4, 200 mM KCl, 0.5% Triton, 1x protease inhibitor, and 1 mM PMSF) and a pestle homogenizer. All the process was conducted on ice. Subsequently, three cycles of freeze and thaw were performed to lyse mitochondria, and brain samples were sonicated for 30 s, intercalated by an interval of 30 s (repeated three times), using an amplitude of 30% (QSONICA sonicator, Newtown, Connecticut, USA). Brain homogenates were then centrifuged once again, this time for 10 min at 18,000×*g* and 4 °C, and supernatants were collected for protein quantification. To conduct the DAPI-polyP assay in murine tissue, we followed our previously published protocol [69]. Samples and standards were assayed in experimental and biological triplicates, and polyP levels were standardized by the levels of the polymer assayed under control conditions. Data is presented as mean ± SEM from at least three biological triplicates and three experimental replicates per samples.

2.14. Transfection with short interfering RNA (siRNA)

To conduct these experiments, we followed our previously published protocol [68]. Briefly, 5×10^5 Wt SH-SY5Y cells/well were seeded on a 6-well plate using antibiotic-free media and incubated for 48 h. $AMPK\alpha_1$ expression was knocked down using $AMPK\alpha_1$ siRNA. To conduct the transfections, 5 μL of lipofectamine 2000 and 100 pmol of siRNA were used. Cells were incubated for 48 h after transfection, before harvesting. The efficiency of the transfections was assayed by immunoblotting to determine the levels of phosphorylated (Thr172) and total AMPK. Scramble siRNA and lipofectamine were used as control conditions.

2.15. Statistical analysis

All experiments were performed using at least three biological replicates. Statistical analysis and graphical representation were performed using GraphPad Prism version 10.2.3 (GraphPad Software, Boston, Massachusetts, USA). An unpaired student t-test was used to compare two groups, and a one-way ANOVA was followed by Tukey's *post hoc*

test for multiple comparisons. Statistical significance was set at $\alpha = 0.05$ ($^{*}p \leq 0.05$, $^{**}p \leq 0.01$, $^{***}p \leq 0.001$, and $^{****}p \leq 0.0001$). All data are expressed as mean ± SEM.

3. RESULTS

To conduct our experiments, we used Wt and stably transfected MitoPPX SH-SY5Y cells. As mentioned in the introduction, MitoPPX SH-SY5Y cells have already been characterized and validated in previous studies, in which it has been demonstrated that the effects of the PPX activity are not due to the transfection procedure *per se*, as well as that the expression of MitoPPX does not significantly increase cell death [13,21,28,82]. However, to further corroborate the lack of effects of the transfection procedure in our results, we used SH-SY5Y cells expressing a mutated version of the MitoPPX construct (^{D127N}MitoPPX SH-SY5Y cells) in some key experiments. This specific mutation impedes substrate recognition by the enzyme, therefore inhibiting its exopolyphosphatase activity [60].

Before conducting our experiments, we corroborated the presence of significantly decreased levels of mitochondrial polyP in MitoPPX cells, when compared to Wt cells (Supplementary Fig. 1A), as well as the presence of PPX in MitoPPX and ^{D127N}MitoPPX cells, but not in the Wt samples (Supplementary Fig. 1B). Lastly, we assayed the enzymatic activity of PPX in all the used cell lines. Our results show that MitoPPX cells have significantly decreased levels of polyP during the time course of the enzymatic assay, while Wt and ^{D127N}MitoPPX cells do not show any significant changes in these levels (Supplementary Fig. 1C).

3.1. Depletion of mitochondrial polyP impairs energy metabolism, independently of changes in content or remodeling indicators

To address the effects of the depletion of mitochondrial polyP on bioenergetics, we measured the oxygen consumption in Wt and MitoPPX cells using Oroboros O2k. Routine respiration and ATP-linked, oligomycin-sensitive respiration were significantly decreased in MitoPPX cells, compared to Wt cells (Figure 1A). The intracellular ATP:ADP ratio was also reduced in those cells (Figure 1B). To eliminate the possibility that these effects could be a direct consequence of differences in mitochondrial mass between Wt and MitoPPX cells, we quantified this parameter using qPCR. Our data show no significant differences in mitochondrial mass between MitoPPX and Wt cells (Figure 1C). Our data also show a lack of differences in the levels of Parkin (mitophagy); and Drp1 and Mitofusin 2 (mitochondrial dynamics) between Wt and MitoPPX cells (Figure 1D). In totality, these findings corroborate most of our previous studies, and they suggest a specific role for polyP in the regulation of mitochondrial bioenergetics and cellular energy balance, via a mechanism yet to be described. The intriguing possibility is that this mechanism could involve the regulation of the phosphorylation of AMPK.

3.2. Decreased AMPK activation, altered Akt signaling, and increased phosphate efflux are present in MitoPPX cells

To study a potential role for polyP in the regulation of the AMPK signaling pathway, we assayed the phosphorylation of AMPKα at T172 (pAMPKα^{T172}), and some main AMPK downstream targets through immunoblot, using whole cells (please note that unless expressly stated, all the experiments included in the Results section were conducted using whole cells). Our data show a significantly decreased pAMPKα^{T172}/AMPK ratio in MitoPPX cells, compared to Wt samples and ^{D127N}MitoPPX cells (Figure 2A). However, our results show no significant differences in the phosphorylation status of some of the downstream targets of AMPK; such as the acetyl-CoA carboxylase (ACC), and the regulatory-associated protein of mTOR (Raptor) (Figure 2B). Moreover, no significant changes are observed in the pAMPK substrate motif immunoblots (Figure 2C).

Subsequently, we examined whether decreased AMPK activity in MitoPPX cells could be mediated via the inhibitory phosphorylation of AMPKα at S485 [83]. However, no significant changes are present in the pAMPKα^{S485}/AMPK ratio between MitoPPX and Wt cells (Figure 2D). Moreover, we assayed the phosphorylation levels of protein kinase B (Akt) in two different sites: T308 and S473. Our results show a significant upregulation in the pAkt^{T308}/Akt ratio, but no significant differences in the pAkt^{S473}/Akt ratio in MitoPPX cells, when compared to the Wt samples (Figure 2E). No significant differences were neither found in the phosphorylation status of a master kinase, the liver kinase B1 (LKB1) (Figure 2F), either in the activity of three different classes of serine/threonine phosphatases: 2A, 2B, and 2C. These latter results suggest that the downregulated phosphorylation of AMPKα^{T172} in MitoPPX cells is not orchestrated by changes in the activity of serine/threonine phosphatases, as reported in previous studies [84–86] (Figure 2G).

Lastly, to explore whether MitoPPX cells have higher intracellular free Pi, we assayed the expression levels of the xenotropic and polytropic retrovirus receptor 1 (XPR1/SLC53A1), a major intracellular mammalian phosphate sensor, located at the plasma membrane [87]. Our results show increased expression of XPR1 in MitoPPX cells, compared to Wt and ^{D127N}MitoPPX cells, suggesting the increased efflux of intracellular free Pi. Subsequently, we examined the expression levels of the inositol hexakisphosphate kinases 1 and 2 (IP6K1 and IP6K2), since both are involved in the positive regulation of XPR1 through the binding of inositol pyrophosphates in the SPX domain of the human phosphate exporter [88]. Our results show increased levels of both IP6K1 and IP6K2 in MitoPPX cells, when compared to Wt samples (Figure 2H).

3.3. Increased amounts of intracellular polyP in SH-SY5Y cells increase AMPKα^{T172} phosphorylation

To determine whether depleted mitochondrial polyP is the cause of the decreased activation of AMPK observed in MitoPPX cells, Wt SH-SY5Y cells were treated with 25 μM of synthetic polyP$_{14}$ for 24 h. This treatment is not cytotoxic to the cells (Supplementary Fig. 2A). Similarly, treatment with sodium phosphate monobasic was conducted to assess the toxicity of Pi, using concentrations that produced comparable or higher levels of Pi than those present when the cells were treated with exogenous polyP. Treatment with sodium phosphate monobasic as a source of Pi has already been used by other authors [89]. Our data show no Pi-induced cytotoxicity in the cells, Figure 2B, as well as that the cells treated with synthetic polyP$_{14}$ have increased levels of intracellular polyP, analyzed by DAPI-polyP spectrophotometric assay. However, no differences were detected in mitochondrial polyP levels in Wt cells (Figure 3A). Subsequently, we assayed the phosphorylation status of AMPKα^{T172} after treatment with synthetic polyP$_{14}$ by immunoblot. Our results show a significant increase in the pAMPK α^{T172}/AMPK ratio in the cells treated with synthetic polyP$_{14}$, compared to the control samples (Figure 3B). Treatment with exogenous polyP$_{14}$ does not affect the protein levels of the main components of the ETC; and of Parkin, Drp1, and Mitofusin 2 (Figure 3C–D).

3.4. AMPKα1 silencing reduces the pAMPKα1^{T172}/AMPK ratio and induces the depletion of polyP

The best-described mechanism of the activation of AMPK is the phosphorylation of T172 of the α subunit [52]. To investigate the effects of AMPKα^{T172} phosphorylation on polyP levels, we used siRNA-mediated knockdown (KD) of AMPKα1 in Wt SH-SY5Y cells. We

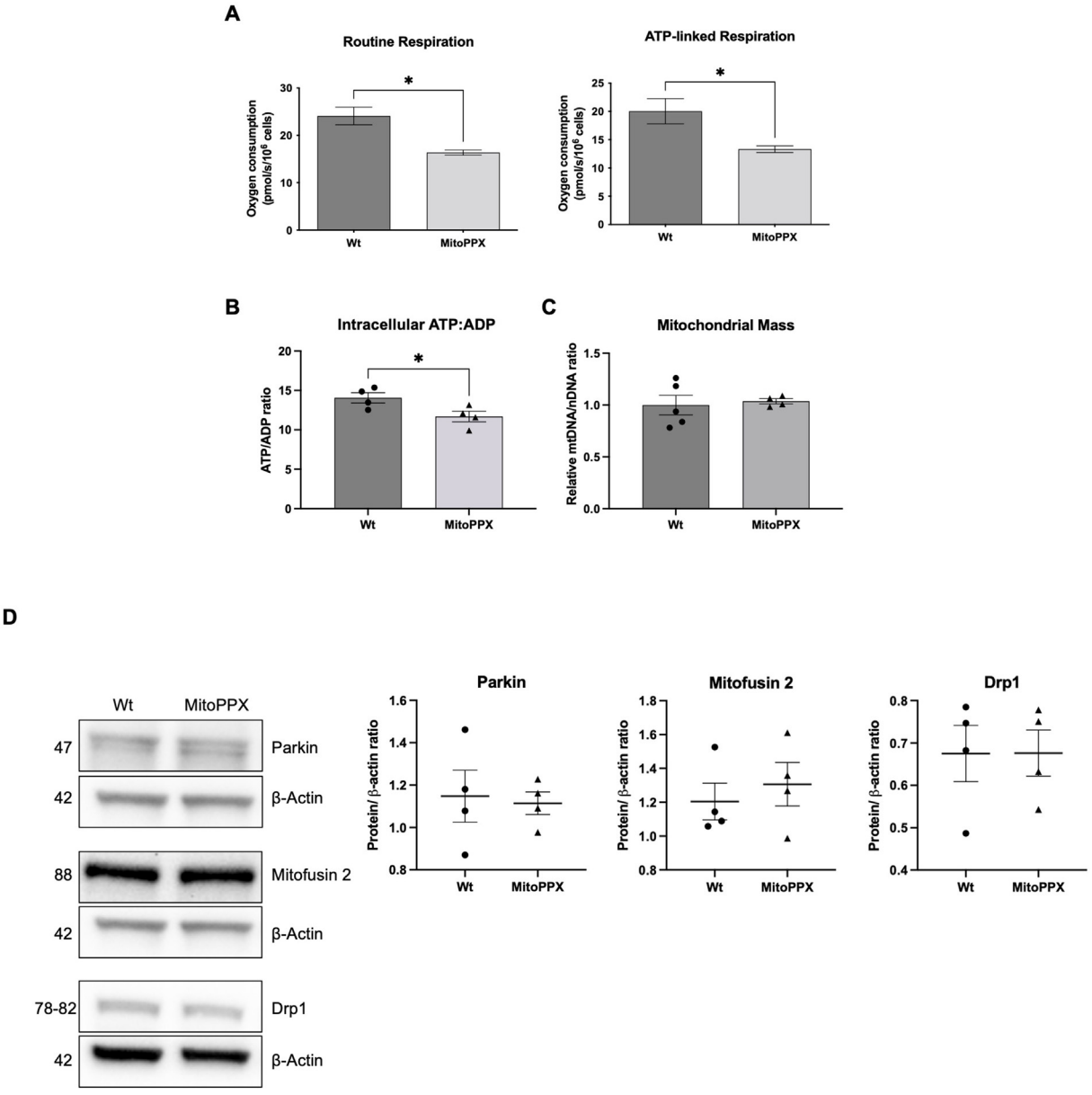

Figure 1: Depletion of mitochondrial polyP dysregulates mammalian energy metabolism. **A.** Oxygen consumption was assayed using Oroboros O2k. Our results show a significant decrease in both routine respiration and ATP-linked respiration in MitoPPX SH-SY5Y cells. **B.** A significant drop in the intracellular ATP:ADP ratio, assayed by HPLC, is present in MitoPPX samples when compared to the Wt SH-SY5Y cells. **C.** qPCR data show no significant effects induced by the mitochondrial depletion of polyP on mitochondrial mass content. **D.** Representative immunoblots and quantification of all the conducted immunoblots, showing the levels of some of the key proteins involved in the maintenance of mammalian mitochondrial physiology (Parkin, Drp1, and Mitofusin 2). No major changes are present in the levels of these proteins between Wt and MitoPPX cells. Some membranes were re-probed with multiple antibodies, and therefore, the same immunoblot showing the signal for β-actin is used for more than one protein. Results are shown as mean ± SEM of at least three independent experiments. $^{*}p \leq 0.05$.

chose to KD this isoform because the modulation of α1, not of α2, has significant effects on brain function, both under healthy and pathological conditions [90,91]. Transfection with the specific siRNA significantly reduces AMPK levels, as well as the pAMPKα1^{T172}/AMPK ratio in SH-SY5Y cells (Figure 4A) without inducing cytotoxicity (Supplementary Fig. 3). In contrast, the non-targeting siRNA does not affect the pAMPKα1^{T172}/AMPK ratio (Figure 4A). Interestingly, the DAPI-polyP assay reveals significantly reduced levels of cellular polyP in the AMPKα1 KD cells, 24 h post-transfection (Figure 4B). Our findings further corroborate the close relationship between the status of AMPK and the levels of polyP.

3.5. The regulatory role of AMPKα1 signaling in polyP metabolism is maintained in the brains of female mice, but not male mice. AMPKα1 loss reveals a gender effect

To address whether AMPKα1 signaling affects the levels of polyP *in vivo*, we assayed the pAMPK/AMPK ratio and the levels of the polymer in brains obtained from AMPKα1^{T172A} knock-in mice, maintained under an *ad libitum* diet. Consistent with previous *in vitro* findings, in the female group, our results show a significant down-regulation in the pAMPK^{T172}/AMPK ratio. Moreover, similarly to the results obtained in cells, decreased AMPK aligns with a significant drop in the levels of polyP in female mice brains. Furthermore, while no

significant differences are present in the phosphorylation status of ACC, a downstream target of AMPK, the expression of total ACC is significantly decreased in these samples (Figure 5A). Remarkably, no significant differences in any of these parameters are present in the brain of knock-in male mice (Figure 5B). These findings suggest a sexual dimorphic effect of AMPKα phosphorylation at the activating site (T172) in maintaining polyP. Specifically, they could be explained by the different abundance of the α1 and α2 isoforms in brains from male and female mice (Figure 5C).

Given the effectiveness of heterozygous AMPKα1^{T172A} knock-in in females, we further assayed the expression of key mitochondrial proteins through immunoblots. Our findings show a significant decrease in the expression of Mitofusin 2, while no significant differences are observed in Parkin, Drp1, and the ETC

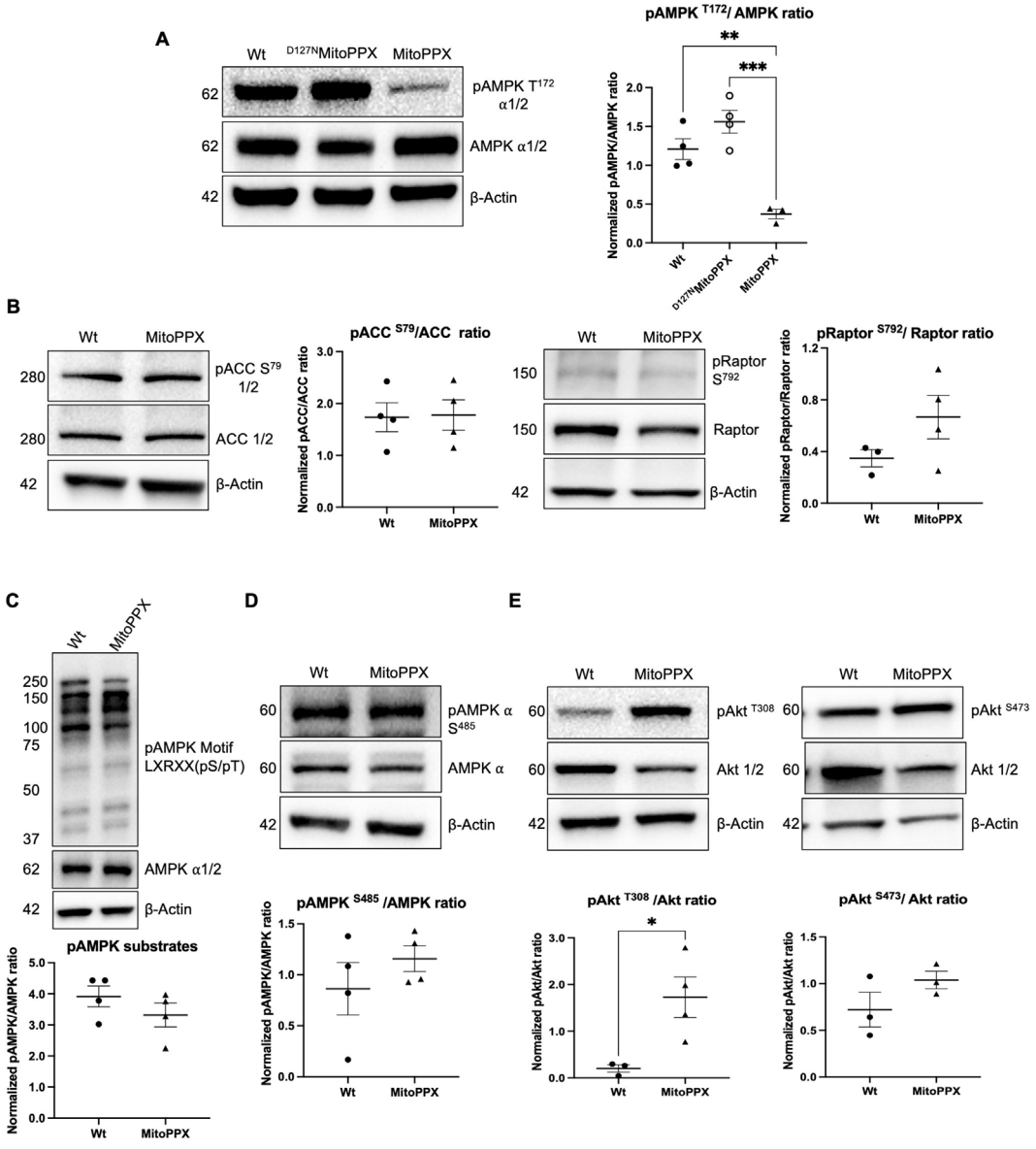

Figure 2: Depletion of mitochondrial polyP reduces the pAMPKα ^{T172}/AMPK ratio, alters Akt signaling, and increases the expression of proteins involved in the Pi efflux pathway. **A.** Representative immunoblots and quantification of all the conducted immunoblots, showing decreased pAMPK ^{T172}/AMPK ratio in MitoPPX SH-SY5Y cells, but no changes in the control ^{D127N}MitoPPX cells. **B.** Representative immunoblots and quantification of all the conducted immunoblots showing no significant differences between Wt and MitoPPX SH-SY5Y cells in the phosphorylation status of ACC at S79 and Raptor at S792, both downstream targets of AMPK. **C.** Representative immunoblots, and quantification of all the conducted immunoblots, showing no significant differences in the pAMPK substrate motif LXRXX(pS/pT) between Wt and MitoPPX SH-SY5Y cells. **D.** Representative immunoblots, and quantification of all the conducted immunoblots, showing no significant differences between Wt and MitoPPX SH-SY5Y cells in the phosphorylation of AMPKα at S485. **E.** Representative immunoblots, and quantification of all the conducted immunoblots, showing increased levels of Akt phosphorylated at T308, but not at S473, in MitoPPX cells, when compared with the Wt samples. **F.** Representative immunoblots, and quantification of all the conducted immunoblots, showing no significant differences between Wt and MitoPPX cells in the pLKB1/LKB1 ratio. **G.** Phosphate activity assays showing no significant differences between Wt and MitoPPX cells for the three main classes of serine/threonine cellular phosphatases (2A, 2B, and 2C). **H.** Representative immunoblots, and quantification of all the conducted immunoblots, showing the upregulation of XPR1(SLC53A1) expression, as well as of IP6K1 and IP6K2, in MitoPPX cells, compared to the Wt samples. Please note that some membranes were re-probed with multiple antibodies, and therefore, the same immunoblot showing the signal for β-actin is used for more than one protein; as well as that protein levels used to calculate the phosphorylated/non phosphorylated protein ratios were previously normalized using β-actin levels. Results are shown as mean ± SEM of at least three independent experiments. $*p \leq 0.05$, $**p \leq 0.01$, $***p \leq 0.001$.

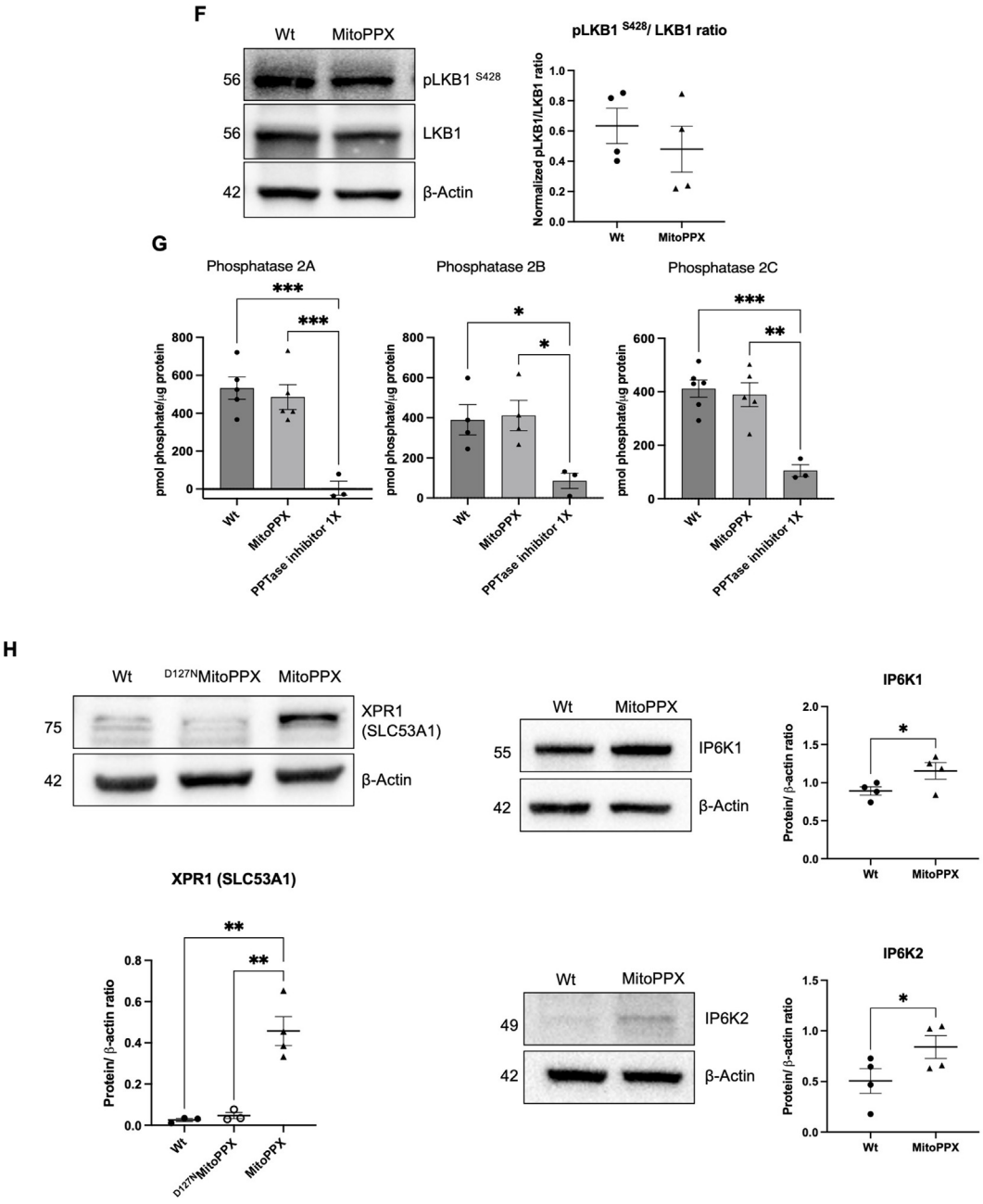

Figure 2: (*continued*).

components (Figure 6A). Consistent with the lack of efficacy in the AMPK$\alpha 1^{T172A}$ knock-in males, no significant differences are present in any of these key mitochondrial proteins in their brains (Supplementary Fig. 4).

4. DISCUSSION

The regulatory role of mitochondrial polyP on energy metabolism has been demonstrated at different levels and in different organisms, including mammalian cells [2,13,14,67]. In fact, previous studies have shown the involvement of polyP in the regulation of many bioenergetics-related physiological functions within mitochondria, including OXPHOS [26,29], via a mechanism yet to be elucidated. For the first time, our results show that intimate crosstalk between the levels of polyP and the activation status of AMPK, which could, at least partially, explain the regulatory effects of polyP on bioenergetics. Moreover, we propose a molecular mechanism underlying this crosstalk, which involves the homeostasis of free Pi. A graphical representation of this proposed mechanism can be found in Figure 7. Using MitoPPX cells, which we have already thoroughly characterized [13,14,25,26,28,29,33,69,70], we first corroborated the deleterious effects of the depletion of mitochondrial polyP on OXPHOS, and we show that the impairment induced by the depletion of mitochondrial polyP on energy metabolism is not linked to significant changes in the

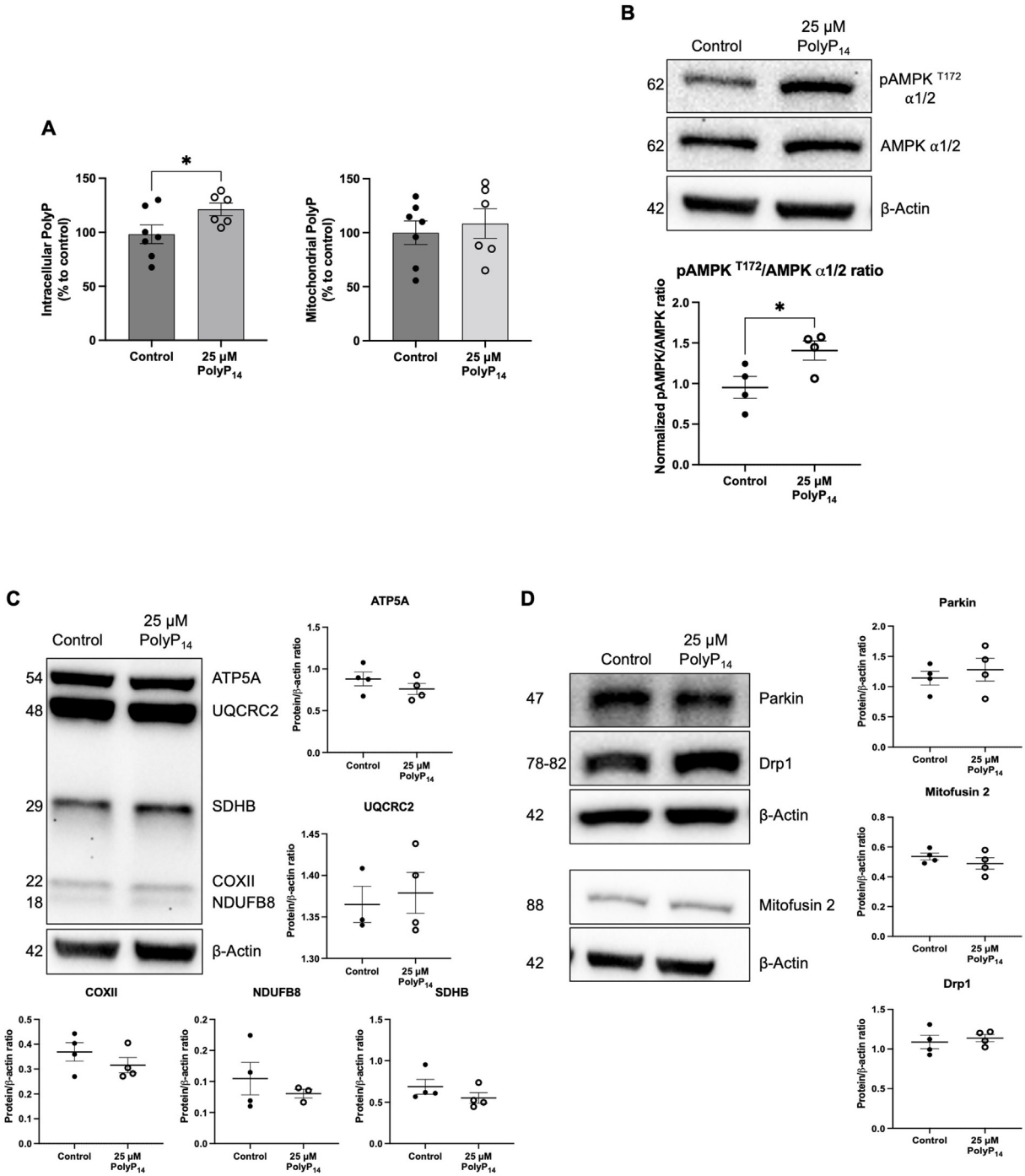

Figure 3: Synthetic polyP$_{14}$ (as sodium salt) treatment increases intracellular levels of polyP in SH-SY5Y cells, leading to an increased pAMPKα^{T172}/AMPK ratio, but without affecting the expression of key proteins involved in mitochondrial physiology. **A.** DAPI-polyP assay showing increased intracellular levels of polyP in polyP$_{14}$-treated cells. However, no significant differences are present in mitochondrial polyP after the treatment with polyP$_{14}$. **B.** Representative immunoblots, and quantification of all the conducted immunoblots, showing the upregulation of AMPKα^{T172} phosphorylation in SH-SY5Y cells treated with 25 µM synthetic sodium polyP$_{14}$ for 24 h. **C.** Representative immunoblots, and quantification of all the conducted immunoblots, showing that the treatment with polyP$_{14}$ does not alter the levels of the protein complexes of the ETC. **D.** Representative immunoblots, and quantification of all the conducted immunoblots, showing that the treatment with polyP$_{14}$ does not alter the levels of some of the main proteins involved in the maintenance of mitochondrial physiology (Parkin, Drp1, and Mitofusin 2). Please note that some membranes were re-probed with multiple antibodies, and therefore, the same immunoblot showing the signal for β-actin is used for more than one protein. Results are shown as mean ± SEM of at least three independent experiments. $^{*}p \leq 0.05$.

number of mitochondria. This last finding corroborates our previous findings [14]. Our data also show that SH-SY5Y cells do not activate the classical stress response as a consequence of dysfunctional OXPHOS, which is aimed to restore energy homeostasis and maintain a functional mitochondrial network, and which involves the regulation of dynamics and mitophagy [71,72,92–95]. In fact, we did not observe any significant effects of the downregulation of AMPK activation on some of the main protein involved in the maintenance of mitochondrial

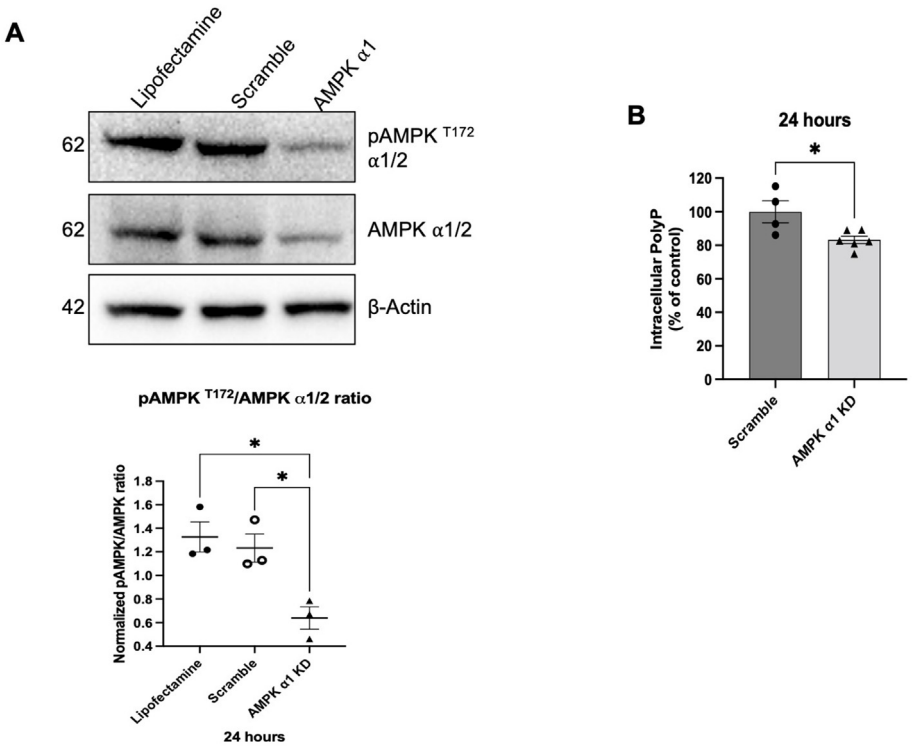

Figure 4: Silencing AMPKα1 reduces the phosphorylation of AMPKα^{T172}, and decreases intracellular levels of polyP. **A.** Representative immunoblot, and quantification of all the conducted immunoblots, showing the results from the siRNA-mediated KD of AMPKα1. Please note the downregulation of the AMPK^{T172} phosphorylation at 24 h post-transfection. **B.** DAPI-polyP quantification showing decreased polyP levels as a consequence of knocking down AMPKα1. Please note that some membranes were re-probed with multiple antibodies, and therefore, the same immunoblot showing the signal for β-actin is used for more than one protein. Results are shown as mean $\pm$ SEM of at least three independent experiments. $^{*}p \leq 0.05$.

mitophagy, fission, and fusion (Parkin, Drp1, and Mitofusin 2, respectively). Although the effects of changes in AMPK activation status on these proteins have been described, the exact crosstalk between AMPK phosphorylation and the status of mitochondrial dynamics and mitophagy still remains far from being fully understood, with high impact research studies showing apparently opposite conclusions [96,97].

The degradation of mitochondrial polyP impairs AMPK activity in SH-SY5Y cells, as determined by the reduced cellular levels of pAMPKα^{T172} (please, note that our studies were conducted including AMPK from all sub-cellular locations). AMPK is a main regulator of mammalian cellular metabolism and mitochondrial homeostasis [46], via sensing variations in the ATP, ADP, and AMP levels, which results in conformational changes and its activation through phosphorylation [98]. Mitochondrial dysfunction deleteriously affects cellular bioenergetics, thus triggering the activation of AMPK to restore energy homeostasis [99]. Interestingly, Pi, which can be stored as polyP [100], is crucially involved in the regulation of the kinase activity of AMPK [101,102], and changes in its levels affect cell physiology [103–107]. Moreover, the hydrolysis of polyP by the PPX enzyme releases orthophosphates [60], which can alter the amount of intracellular Pi, closing the regulatory feedback. The molecular mechanisms involved in the efflux of Pi from mitochondria to cytosol still remain poorly understood, even though the role of the DIC/SLC25A10 carrier has already been proposed in this process [108].

Our findings show an upregulation of the cytosolic levels of XPR1, as well as of IP6K1 and IP6K2, in MitoPPX cells. XPR1 functions as a Pi exporter, sensing the intracellular levels of Pi via the SPX domain [87]. Moreover, IP6K1 and IP6K2 can modulate the intracellular concentration of 5-diphosphoinositol pentakisphosphate 7 (5-IP_7) in response to changes in the intracellular levels of Pi [88]. Changes in the concentration of 5-IP_7 have been demonstrated to trigger a molecular response to restore the intracellular levels of Pi by activating the XPR1-mediated Pi efflux [88]. The increased levels of all these proteins in MitoPPX cells suggest the presence of intracellular Pi dyshomeostasis as a consequence of the activity of the PPX enzyme. It also indirectly implies an increase in inositol levels [88,109,110]. Notably, inositol was recently reported to act as an endogenous inhibitor of AMPK activity, thus affecting mitochondrial physiology [48]. In fact, our findings show that even when the ATP:ADP ratio is decreased in MitoPPX cells, AMPK activation is not triggered, which aligns with previous results showing that unbalanced levels of inositol impact the AMPK activity, independently of the levels of ATP [48]. In our previous studies, no significant differences in cell growth were observed between Wt and MitoPPX cells at the time points when the experiments presented in this manuscript were conducted [70]. This lack of differences rules out the possibility that MitoPPX cells enter a dormant state, which would otherwise impact AMPK activation and bioenergetic status.

The large suppression of the activity of AMPK in MitoPPX cells seems to have none or only limited effects on the phosphorylation of some of the best-known downstream targets of the enzyme, such as pACC and pRaptor; as well as the phosphorylation of specific motifs aimed by pAMPK in its substrates. These results suggest a non-ATP:ADP ratio-dependent mechanism involved in the modulation of the AMPK activity in MitoPPX cells; therefore, probably explaining the lack of observed effects

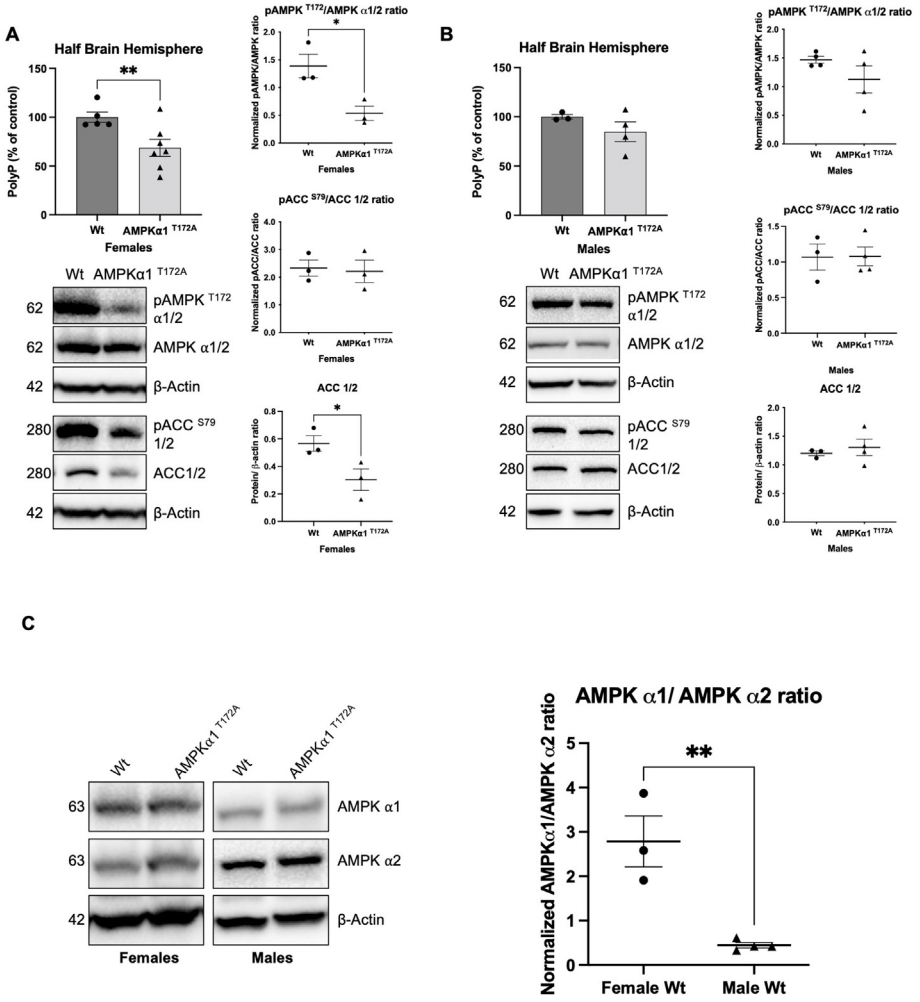

Figure 5: Decreased levels of polyP and pAMPKα^{T172}/AMPK ratio are present in the brain of AMPKα1 knock-in female mice but not in males. **A**. DAPI-polyP assay showing decreased levels of polyP in the brain of AMPKα1 knock-in female mice, maintained on an *ad libitum* diet. Representative immunoblots, and quantification of all the conducted immunoblots, characterizing the levels of pAMPK^{T172}, AMPK, and ACC in the same tissue. **B.** DAPI-polyP assay showing decreased levels of polyP in the brain of AMPKα1 knock-in male mice, maintained on an *ad libitum* diet. Representative immunoblots, and quantification of all the conducted immunoblots, characterizing the levels of pAMPK^{T172}, AMPK, and ACC in the same tissue. **C.** Representative immunoblots, and quantification of all the conducted immunoblots, comparing the abundance of AMPKα isoforms in the brain of female and male mice. Data is shown as ratio of the α1/α2 isoforms. Please note that some membranes were re-probed with multiple antibodies, and therefore, the same immunoblot showing the signal for β-actin is used for more than one protein. Results are shown as mean ± SEM of at least three independent experiments. $*p \leq 0.05$, $**p \leq 0.01$, and $****p \leq 0.0001$.

in the classical downstream targets. Mechanistically, T172 phosphorylation of AMPK has been described as an essential step for the phosphorylation of these downstream targets, including the two that we addressed in this study [111]. Only allosteric activation has been described as a sufficient mechanism, independent of the T172 phosphorylation, even if this has never been demonstrated in live cells before [112]. Therefore, our results suggest either the existence of a new mechanism of control of AMPK activity, which circumvents the requirement for downstream phosphorylation when T172 is phosphorylated; or that the observed effects in the phosphorylation of AMPK are transient, while those on the substrates are preserved for a longer time. Previous studies have shown that AMPK and Akt play antagonistic roles. Akt possesses two phosphorylation sites (Thr308 and Ser473) that are related to its full activation [113–116]. Once it is fully activated, under certain conditions, Akt phosphorylates multiple downstream targets, including AMPKα^{S485} (Ser485 is an inhibitory site of AMPK [83,117,118]), ultimately contributing to the suppression of AMPKα activity [83]. Our findings show that the downregulation of pAMPKα^{T172} is not mediated by the full activation of Akt. However, the phosphorylation of Akt in the residue Thr308, but not Ser473, is increased in MitoPPX cells compared to Wt samples. Remarkably, the increased phosphorylation of this specific site of Akt has been reported as an upstream activator for the transduction of signals evoked by the excess of intracellular free Pi in the human lung [119]. Therefore, the increased levels of pAkt^{T308} observed in MitoPPX cells could correlate with the increased intracellular free Pi produced by the degradation of polyP, which could ultimately induce a signal transduction response suppressing pAMPKα^{T172}. Supporting this, our findings also exclude the plausible negative effects of LKB1, which is a main upstream regulator of AMPK; and the dysfunction of the serine/threonine phosphatase activity. Both processes can also orchestrate the suppression of the phosphorylation of AMPKα at T172 [84,85,120].

To further describe the crosstalk between polyP and AMPK signaling, we addressed the effects of treatment with synthetic polyP, as well as knocking down AMPKα1, in SH-SY5Y cells. Treatment with exogenous polyP has already been previously used by other authors to conduct

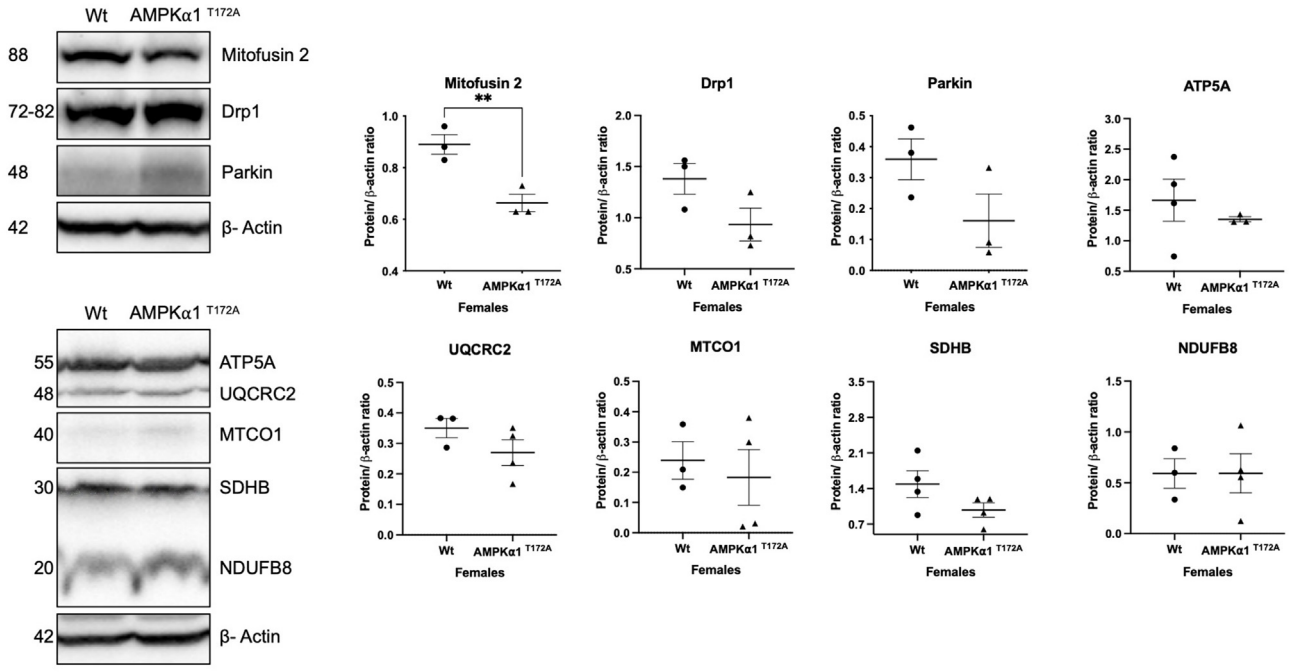

Figure 6: Abundance of some key proteins involved in the regulation of mitochondrial physiology in the brain of AMPKα1 knock-in females. Representative immunoblots, and quantification of all the conducted immunoblots of some of the key proteins involved in the maintenance of mitochondrial physiology (Mitofusin 2, Drp1, Parkin, and ETC complexes). Experiments were conducted using brain tissue from the animals. Please note that some membranes were re-probed with multiple antibodies, and therefore, the same immunoblot showing the signal for β-actin is used for more than one protein. Results are shown as mean ± SEM of at least three independent experiments. $^{**}p \leq 0.01$.

in vivo experiments [2,34,121]. Our data show that this treatment rapidly increases the cellular levels of the polymer, suggesting that at least a part of polyP was not degraded. This aligns with the bibliography in the field, which did not report major degradation of the polymer after treatment [2,34,121], even though increased secretion of extracellular vesicles containing alkaline phosphatase was reported by a group of authors who conducted their studies using SaOS-2 cells [2]. Our data also show that mitochondrial levels of polyP are not affected by this treatment with exogenous polyP. This finding can be explained in the context of the strong calcium homeostasis system present in the

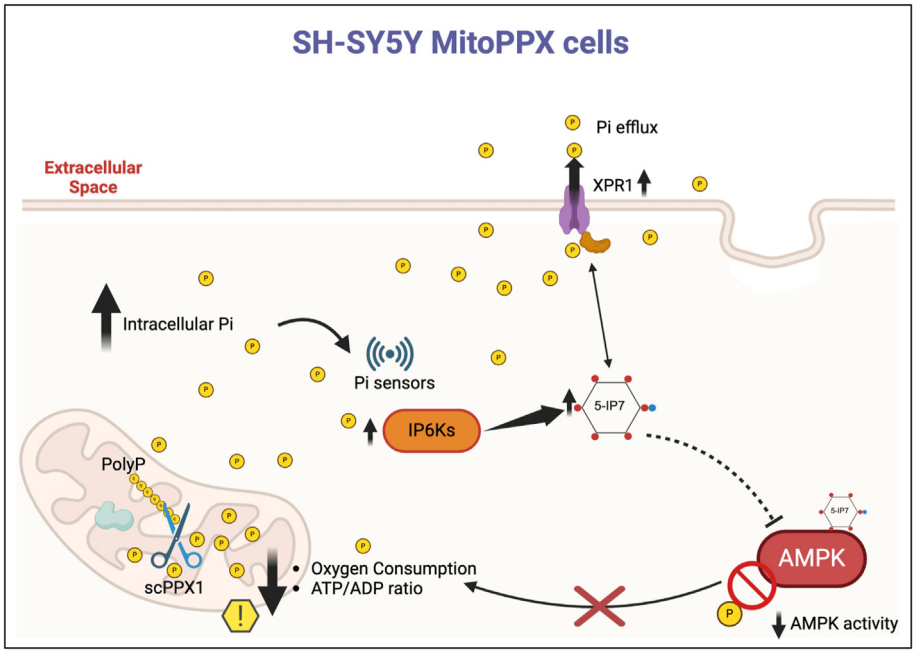

Figure 7: Graphical representation of the proposed molecular mechanism. This figure provides a graphical summary of the findings presented in this manuscript, derived from experiments conducted using SH-SY5Y cells. For space efficiency, individual free phosphates are represented as yellow circles and abbreviated as "P" throughout the figure. This representation was created using BioRender and an institutional license to Rutgers University.

organelle, which could be mediated, at least partially, by polyP. Interestingly, our previous work already demonstrated the high affinity of polyP for mitochondrial free calcium, acting as a buffer [14,25]. Accordingly, increased polyP could bind to calcium; therefore affecting its detection. Furthermore, the limited understanding of the mechanisms involved in mitochondrial polyP import makes it difficult to hypothesize whether changes in energy status could also influence this process.

Our data show that increased polyP positively regulates the phosphorylation of AMPK, while decreased AMPK phosphorylation leads to lower intracellular polyP levels. These findings could be interpreted as an attempt of the cell to maintain bioenergetics. Downregulated AMPK is closely related to decreased basal energy homeostasis [40,122]. Therefore, under this experimental scenario and with the aim of maintaining appropriate ATP/ADP balance, the cell could trigger the degradation of polyP. Similar to what we observed in the experiments conducted using Wt and MitoPPX cells under control conditions, also in this case we do not observe a major relationship between the activation of AMPK and the status of mitochondrial dynamics and mitophagy. As mentioned above, the bibliography is contradictory regarding the effects of AMPK activation on mitophagy and dynamics [96,97], and more studies should be conducted to better describe this relationship.

We also explored the role of mitochondrial polyP in the regulation of AMPK signaling using brains from mice lacking AMPK$\alpha1^{T172}$ phosphorylation. In this case, we observed a downregulation of pAMPK$\alpha1^{T172}$/AMPK which correlates with lower levels of polyP in the brains of female mice, but not in male mice. In the same samples from females, we found significantly decreased levels of Mitofusin 2, which suggests a downstream effect of the loss of pAMPK$\alpha1^{T172}$. Notably, the effects on Mitofusin 2 are not observed in MitoPPX cells, which we attributed to the specific cellular model that we decided to use, as well as to the experimental conditions. In fact, Mitofusin 2 is not homogenously distributed in the different mammalian cells [123], and the levels of serum can affect its expression [124]. Therefore, the changes in the crosstalk between polyP and Mitofusin 2 could have varying effects depending on the specific type of samples and the growth conditions (please, note the major differences in these two parameters between SH-SY5Y cells and brain tissue). Similar results were observed in ACC expression (which is one of the main downstream targets of AMPK). Specifically, decreased ACC is present in female mice that lack pAMPK$\alpha1^{T172}$; however, as mentioned above, no differences are present in this parameter when assayed in MitoPPX cells. These discrepancies could be explained by considering the distinct mechanisms that suppress pAMPK$\alpha1^{T172}$ in these two models. Specifically, in MitoPPX cells, this suppression seems to be a consequence of the changes in Pi levels, subsequent to the activity of the PPX enzyme. However, this suppression in mice is a consequence of direct genetic manipulation in the activation site of the enzyme. It is our understanding that the use of the different strategies enhances the validity of our results regarding the crosstalk between AMPK status and polyP levels, while acknowledging potential differences in other results.

Also, our findings show significant sex-specific differences in the isoforms of AMPK that are activated in the murine brain. Specifically, in female mice, AMPK$\alpha1$ is the largely predominant α isoform (which is the same isoform present in SH-SY5Y cells), while in male mice this is AMPK$\alpha2$. Interestingly, SH-SY5Y cells were obtained from a female donor [125]. This could support the observed differences between the results in the two genders, and they highlight the need for further research into the effects of sex in AMPK metabolism and regulation in the mammalian brain. In these samples, we did not address the status of Akt since changes in AMPK were genetically induced in the mice. The scope of our studies regarding the study of Akt in SH-SY5Y cells was to address whether changes in this protein status could be mechanistically involved in the suppression of the activity of AMPK.

In summary, our study demonstrates for the first time the crosstalk between the levels of mitochondrial polyP and the activation status of AMPK. Our results also suggest that this role is mediated by Pi homeostasis. The crosstalk between polyP levels and AMPK metabolism seems to be conserved from cells to female murine brains. Accordingly, our results could pave the way for the use of the metabolism of polyP as a valid and innovative pharmacological target in many diseases where bioenergetics dysregulation has been broadly described. These diseases range from neurodegenerative disorders [126–128], to COVID [128], and cancer [129]. Interestingly, some authors have already demonstrated that modifying polyP levels has positive effects in the field of hematology. For example, inhibition of polyP has shown to be a valid strategy for preventing thrombosis and inflammation [130], and neutralization of blood-borne polyP provides thromboprotection [131]. Monoclonal antibodies against polyP have already been obtained from mice [132], which opens new and exciting possibilities in the field of polyP. However, some further questions will have to be answered to increase the scenarios in which the metabolism of polyP could be used as a pharmacological target, especially when targeting bioenergetics dysregulation. These questions include, for example, which molecular mechanisms are used for sensing and allowing the different pools of polyP and Pi to communicate within the mammalian cell; as well as which enzymes are involved in the mammalian metabolism of polyP.

CRediT AUTHORSHIP CONTRIBUTION STATEMENT

Renata T. Da Costa: Writing — review & editing, Writing — original draft, Validation, Methodology, Investigation, Formal analysis, Conceptualization. **Anna Nichenko:** Resources, Investigation. **Matheus M. Perez:** Methodology, Investigation. **Malgorzata Tokarska-Schlattner:** Methodology, Investigation. **Sheida Kavehmoghaddam:** Methodology, Investigation. **Vedangi Hambardikar:** Methodology, Investigation. **Ernest R. Scoma:** Methodology, Investigation. **Erin L. Seifert:** Writing — review & editing, Methodology, Investigation, Conceptualization. **Uwe Schlattner:** Writing — review & editing, Methodology, Investigation, Conceptualization. **Joshua C. Drake:** Writing — review & editing, Resources, Methodology, Investigation, Conceptualization. **Maria E. Solesio:** Writing — review & editing, Writing — original draft, Supervision, Resources, Project administration, Methodology, Funding acquisition, Conceptualization.

ACKNOWLEDGEMENTS

We kindly thank Dr. Toshikazu Shiba from Kitasato University (Tokyo, Japan) for kindly providing us with synthetic polyP; as well as Dr. James H. Morrissey and Dr. Stephanie A. Smith from the University of Michigan (Michigan, USA) for kindly providing us with the scPPX enzyme. Lastly, we thank Mitch Maleki, Esq. for editing the manuscript.

FUNDING

This project was funded by an R35 grant (835813) from the NIH and, an AHA Career Development Award (830530) to MES; as well as by an R00 (057825), and an R01 grants (080731), both from the NIH, to JCD;

and an R01 grant (1DK138011) from the NIH to ELS. The stipend of Dr. Torres Da Costa was supported with a Supplement to Increase Diversity for MES' AHA grant, awarded to RTDC (833054).

DECLARATION OF COMPETING INTEREST

The authors declare no conflict of interests.

APPENDIX A. SUPPLEMENTARY DATA

Supplementary data to this article can be found online at https://doi.org/10.1016/j.molmet.2024.102077.

DATA AVAILABILITY

Data will be made available on request. Uncropped membranes from all the immunoblots are included as Supplementary Materials.

REFERENCES

[1] Kornberg A. Inorganic polyphosphate: a molecule of many functions. Prog Mol Subcell Biol 1999;23:1—18. https://doi.org/10.1007/978-3-642-58444-2_1.

[2] Muller WEG, Wang S, Neufurth M, Kokkinopoulou M, Feng Q, Schroder HC, et al. Polyphosphate as a donor of high-energy phosphate for the synthesis of ADP and ATP. J Cell Sci 2017;130:2747—56. https://doi.org/10.1242/jcs.204941.

[3] Muller WEG, Schroder HC, Wang X. Inorganic polyphosphates as storage for and generator of metabolic energy in the extracellular matrix. Chem Rev 2019;119:12337—74. https://doi.org/10.1021/acs.chemrev.9b00460.

[4] Khong ML, Li L, Solesio ME, Pavlov EV, Tanner JA. Inorganic polyphosphate controls cyclophilin B-mediated collagen folding in osteoblast-like cells. FEBS J 2020;287:4500—24. https://doi.org/10.1111/febs.15249.

[5] Kim KS, Rao NN, Fraley CD, Kornberg A. Inorganic polyphosphate is essential for long-term survival and virulence factors in Shigella and Salmonella spp. Proc Natl Acad Sci U S A 2002;99:7675—80. https://doi.org/10.1073/pnas.112210499.

[6] Kornberg A, Rao NN, Ault-Riche D. Inorganic polyphosphate: a molecule of many functions. Annu Rev Biochem 1999;68:89—125. https://doi.org/10.1146/annurev.biochem.68.1.89.

[7] Rabinowitz J, Chang S, Ponnamperuma C. Phosphorylation by way of inorganic phosphate as a potential prebiotic process. Nature 1968;218:442—3. https://doi.org/10.1038/218442a0.

[8] Westheimer FH. Why nature chose phosphates. Science 1987;235:1173—8. https://doi.org/10.1126/science.2434996.

[9] Kamerlin SC, Sharma PK, Prasad RB, Warshel A. Why nature really chose phosphate. Q Rev Biophys 2013;46:1—132. https://doi.org/10.1017/S0033583512000157.

[10] Lynn WS, Brown RH. Synthesis of polyphosphate by rat liver mitochondria. Biochem Biophys Res Commun 1963;11:367—71. https://doi.org/10.1016/0006-291x(63)90124-4.

[11] Gabel NW, Thomas V. Evidence for the occurrence and distribution of inorganic polyphosphates in vertebrate tissues. J Neurochem 1971;18:1229—42. https://doi.org/10.1111/j.1471-4159.1971.tb00222.x.

[12] Angelova PR, Iversen KZ, Teschemacher AG, Kasparov S, Gourine AV, Abramov AY. Signal transduction in astrocytes: localization and release of inorganic polyphosphate. Glia 2018;66:2126—36. https://doi.org/10.1002/glia.23466.

[13] Abramov AY, Fraley C, Diao CT, Winkfein R, Colicos MA, Duchen MR, et al. Targeted polyphosphatase expression alters mitochondrial metabolism and inhibits calcium-dependent cell death. Proc Natl Acad Sci U S A 2007;104:18091—6. https://doi.org/10.1073/pnas.0708959104.

[14] Solesio ME, Demirkhanyan L, Zakharian E, Pavlov EV. Contribution of inorganic polyphosphate towards regulation of mitochondrial free calcium. Biochim Biophys Acta 2016;1860:1317—25. https://doi.org/10.1016/j.bbagen.2016.03.020.

[15] Solesio ME, Elustondo PA, Zakharian E, Pavlov EV. Inorganic polyphosphate (polyP) as an activator and structural component of the mitochondrial permeability transition pore. Biochem Soc Trans 2016;44:7—12. https://doi.org/10.1042/BST20150206.

[16] Kumble KD, Kornberg A. Inorganic polyphosphate in mammalian cells and tissues. J Biol Chem 1995;270:5818—22. https://doi.org/10.1074/jbc.270.11.5818.

[17] Borghi F, Azevedo C, Johnson E, Burden JJ, Saiardi A. A mammalian model reveals inorganic polyphosphate channeling into the nucleolus and induction of a hyper-condensate state. Cell Rep Method 2024;4:100814. https://doi.org/10.1016/j.crmeth.2024.100814.

[18] Ruiz FA, Lea CR, Oldfield E, Docampo R. Human platelet dense granules contain polyphosphate and are similar to acidocalcisomes of bacteria and unicellular eukaryotes. J Biol Chem 2004;279:44250—7. https://doi.org/10.1074/jbc.M406261200.

[19] Muller WEG, Wang S, Wiens M, Neufurth M, Ackermann M, Relkovic D, et al. Uptake of polyphosphate microparticles *in vitro* (SaOS-2 and HUVEC cells) followed by an increase of the intracellular ATP pool size. PLoS One 2017;12:e0188977. https://doi.org/10.1371/journal.pone.0188977.

[20] Freimoser FM, Hurlimann HC, Jakob CA, Werner TP, Amrhein N. Systematic screening of polyphosphate (poly P) levels in yeast mutant cells reveals strong interdependence with primary metabolism. Genome Biol 2006;7:R109. https://doi.org/10.1186/gb-2006-7-11-r109.

[21] Seidlmayer LK, Juettner VV, Kettlewell S, Pavlov EV, Blatter LA, Dedkova EN. Distinct mPTP activation mechanisms in ischaemia-reperfusion: contributions of Ca2+, ROS, pH, and inorganic polyphosphate. Cardiovasc Res 2015;106:237—48. https://doi.org/10.1093/cvr/cvv097.

[22] Suess PM, Watson J, Chen W, Gomer RH. Extracellular polyphosphate signals through Ras and Akt to prime Dictyostelium discoideum cells for development. J Cell Sci 2017;130:2394—404. https://doi.org/10.1242/jcs.203372.

[23] Muller WEG, Wang S, Ackermann M, Neufurth M, Steffen R, Mecja E, et al. Rebalancing beta-amyloid-induced decrease of ATP level by amorphous nano/micro polyphosphate: suppression of the neurotoxic effect of amyloid beta-protein fragment 25-35. Int J Mol Sci 2017;18. https://doi.org/10.3390/ijms18102154.

[24] Seidlmayer LK, Gomez-Garcia MR, Shiba T, Porter Jr GA, Pavlov EV, Bers DM, et al. Dual role of inorganic polyphosphate in cardiac myocytes: the importance of polyP chain length for energy metabolism and mPTP activation. Arch Biochem Biophys 2019;662:177—89. https://doi.org/10.1016/j.abb.2018.12.019.

[25] Solesio ME, Garcia Del Molino LC, Elustondo PA, Diao C, Chang JC, Pavlov EV. Inorganic polyphosphate is required for sustained free mitochondrial calcium elevation, following calcium uptake. Cell Calcium 2020;86:102127. https://doi.org/10.1016/j.ceca.2019.102127.

[26] Guitart-Mampel M, Urquiza P, Carnevale Neto F, Anderson JR, Hambardikar V, Scoma ER, et al. Mitochondrial inorganic polyphosphate (polyP) is a potent regulator of mammalian bioenergetics in SH-SY5Y cells: a proteomics and metabolomics study. Front Cell Dev Biol 2022;10:833127. https://doi.org/10.3389/fcell.2022.833127.

[27] Borden EA, Furey M, Gattone NJ, Hambardikar VD, Liang XH, Scoma ER, et al. Is there a link between inorganic polyphosphate (polyP), mitochondria, and neurodegeneration? Pharmacol Res 2021;163:105211. https://doi.org/10.1016/j.phrs.2020.105211.

[28] Hambardikar V, Guitart-Mampel M, Scoma ER, Urquiza P, Nagana GGA, Raftery D, et al. Enzymatic depletion of mitochondrial inorganic

polyphosphate (polyP) increases the generation of reactive oxygen species (ROS) and the activity of the pentose phosphate pathway (PPP) in mammalian cells. Antioxidants 2022;11:11. https://doi.org/10.3390/antiox11040685.

[29] Solesio ME, Xie L, McIntyre B, Ellenberger M, Mitaishvili E, Bhadra-Lobo S, et al. Depletion of mitochondrial inorganic polyphosphate (polyP) in mammalian cells causes metabolic shift from oxidative phosphorylation to glycolysis. Biochem J 2021;478:1631–46. https://doi.org/10.1042/BCJ20200975.

[30] Gray MJ, Wholey WY, Wagner NO, Cremers CM, Mueller-Schickert A, Hock NT, et al. Polyphosphate is a primordial chaperone. Mol Cell 2014;53:689–99. https://doi.org/10.1016/j.molcel.2014.01.012.

[31] Cremers CM, Knoefler D, Gates S, Martin N, Dahl JU, Lempart J, et al. Polyphosphate: a conserved modifier of amyloidogenic processes. Mol Cell 2016;63:768–80. https://doi.org/10.1016/j.molcel.2016.07.016.

[32] Yoo NG, Dogra S, Meinen BA, Tse E, Haefliger J, Southworth DR, et al. Polyphosphate stabilizes protein unfolding intermediates as soluble amyloid-like oligomers. J Mol Biol 2018;430:4195–208. https://doi.org/10.1016/j.jmb.2018.08.016.

[33] Da Costa RT, Urquiza P, Perez MM, Du Y, Khong ML, Zheng H, et al. Mitochondrial inorganic polyphosphate is required to maintain proteostasis within the organelle. Front Cell Dev Biol 2024;12:1423208. https://doi.org/10.3389/fcell.2024.1423208.

[34] Holmstrom KM, Marina N, Baev AY, Wood NW, Gourine AV, Abramov AY. Signalling properties of inorganic polyphosphate in the mammalian brain. Nat Commun 2013;4:1362. https://doi.org/10.1038/ncomms2364.

[35] Arredondo C, Cefaliello C, Dyrda A, Jury N, Martinez P, Diaz I, et al. Excessive release of inorganic polyphosphate by ALS/FTD astrocytes causes non-cell-autonomous toxicity to motoneurons. Neuron 2022;110:1656–70. https://doi.org/10.1016/j.neuron.2022.02.010. e1612.

[36] Bae JS, Lee W, Rezaie AR. Polyphosphate elicits pro-inflammatory responses that are counteracted by activated protein C in both cellular and animal models. J Thromb Haemostasis 2012;10:1145–51. https://doi.org/10.1111/j.1538-7836.2012.04671.x.

[37] Dinarvand P, Hassanian SM, Qureshi SH, Manithody C, Eissenberg JC, Yang L, et al. Polyphosphate amplifies proinflammatory responses of nuclear proteins through interaction with receptor for advanced glycation end products and P2Y1 purinergic receptor. Blood 2014;123:935–45. https://doi.org/10.1182/blood-2013-09-529602.

[38] Hassanian SM, Dinarvand P, Smith SA, Rezaie AR. Inorganic polyphosphate elicits pro-inflammatory responses through activation of the mammalian target of rapamycin complexes 1 and 2 in vascular endothelial cells. J Thromb Haemostasis 2015;13:860–71. https://doi.org/10.1111/jth.12899.

[39] Ward PS, Thompson CB. Signaling in control of cell growth and metabolism. Cold Spring Harbor Perspect Biol 2012;4:a006783. https://doi.org/10.1101/cshperspect.a006783.

[40] Jeon SM. Regulation and function of AMPK in physiology and diseases. Exp Mol Med 2016;48:e245. https://doi.org/10.1038/emm.2016.81.

[41] Mihaylova MM, Shaw RJ. The AMPK signalling pathway coordinates cell growth, autophagy and metabolism. Nat Cell Biol 2011;13:1016–23. https://doi.org/10.1038/ncb2329.

[42] Rabinovitch RC, Samborska B, Faubert B, Ma EH, Gravel SP, Andrzejewski S, et al. AMPK maintains cellular metabolic homeostasis through regulation of mitochondrial reactive oxygen species. Cell Rep 2017;21:1–9. https://doi.org/10.1016/j.celrep.2017.09.026.

[43] Hawley SA, Davison M, Woods A, Davies SP, Beri RK, Carling D, et al. Characterization of the AMP-activated protein kinase kinase from rat liver and identification of threonine 172 as the major site at which it phosphorylates AMP-activated protein kinase. J Biol Chem 1996;271:27879–87. https://doi.org/10.1074/jbc.271.44.27879.

[44] Crute BE, Seefeld K, Gamble J, Kemp BE, Witters LA. Functional domains of the alpha1 catalytic subunit of the AMP-activated protein kinase. J Biol Chem 1998;273:35347–54. https://doi.org/10.1074/jbc.273.52.35347.

[45] Stein SC, Woods A, Jones NA, Davison MD, Carling D. The regulation of AMP-activated protein kinase by phosphorylation. Biochem J 2000;345(Pt 3):437–43.

[46] Herzig S, Shaw RJ. AMPK: guardian of metabolism and mitochondrial homeostasis. Nat Rev Mol Cell Biol 2018;19:121–35. https://doi.org/10.1038/nrm.2017.95.

[47] Bang S, Kim S, Dailey MJ, Chen Y, Moran TH, Snyder SH, et al. AMP-activated protein kinase is physiologically regulated by inositol polyphosphate multikinase. Proc Natl Acad Sci U S A 2012;109:616–20. https://doi.org/10.1073/pnas.1119751109.

[48] Hsu CC, Zhang X, Wang G, Zhang W, Cai Z, Pan BS, et al. Inositol serves as a natural inhibitor of mitochondrial fission by directly targeting AMPK. Mol Cell 2021;81:3803–19. https://doi.org/10.1016/j.molcel.2021.08.025. e3807.

[49] Liang J, Xu ZX, Ding Z, Lu Y, Yu Q, Werle KD, et al. Myristoylation confers noncanonical AMPK functions in autophagy selectivity and mitochondrial surveillance. Nat Commun 2015;6:7926. https://doi.org/10.1038/ncomms8926.

[50] Drake JC, Wilson RJ, Laker RC, Guan Y, Spaulding HR, Nichenko AS, et al. Mitochondria-localized AMPK responds to local energetics and contributes to exercise and energetic stress-induced mitophagy. Proc Natl Acad Sci U S A 2021;118. https://doi.org/10.1073/pnas.2025932118.

[51] Afinanisa Q, Cho MK, Seong HA. AMPK localization: a key to differential energy regulation. Int J Mol Sci 2021;22. https://doi.org/10.3390/ijms222010921.

[52] Hardie DG, Ross FA, Hawley SA. AMPK: a nutrient and energy sensor that maintains energy homeostasis. Nat Rev Mol Cell Biol 2012;13:251–62. https://doi.org/10.1038/nrm3311.

[53] Bando H, Atsumi T, Nishio T, Niwa H, Mishima S, Shimizu C, et al. Phosphorylation of the 6-phosphofructo-2-kinase/fructose 2,6-bisphosphatase/PFKFB3 family of glycolytic regulators in human cancer. Clin Cancer Res 2005;11:5784–92. https://doi.org/10.1158/1078-0432.CCR-05-0149.

[54] Marsin AS, Bertrand L, Rider MH, Deprez J, Beauloye C, Vincent MF, et al. Phosphorylation and activation of heart PFK-2 by AMPK has a role in the stimulation of glycolysis during ischaemia. Curr Biol 2000;10:1247–55. https://doi.org/10.1016/s0960-9822(00)00742-9.

[55] Yao J, Irwin RW, Zhao L, Nilsen J, Hamilton RT, Brinton RD. Mitochondrial bioenergetic deficit precedes Alzheimer's pathology in female mouse model of Alzheimer's disease. Proc Natl Acad Sci U S A 2009;106:14670–5. https://doi.org/10.1073/pnas.0903563106.

[56] Le A, Cooper CR, Gouw AM, Dinavahi R, Maitra A, Deck LM, et al. Inhibition of lactate dehydrogenase A induces oxidative stress and inhibits tumor progression. Proc Natl Acad Sci U S A 2010;107:2037–42. https://doi.org/10.1073/pnas.0914433107.

[57] Qin C, Yang S, Chu YH, Zhang H, Pang XW, Chen L, et al. Signaling pathways involved in ischemic stroke: molecular mechanisms and therapeutic interventions. Signal Transduct Targeted Ther 2022;7:215. https://doi.org/10.1038/s41392-022-01064-1.

[58] Kumble KD, Kornberg A. Endopolyphosphatases for long chain inorganic polyphosphate in yeast and mammals. J Biol Chem 1996;271:27146–51. https://doi.org/10.1074/jbc.271.43.27146.

[59] Sethuraman A, Rao NN, Kornberg A. The endopolyphosphatase gene: essential in Saccharomyces cerevisiae. Proc Natl Acad Sci U S A 2001;98:8542–7. https://doi.org/10.1073/pnas.151269398.

[60] Ugochukwu E, Lovering AL, Mather OC, Young TW, White SA. The crystal structure of the cytosolic exopolyphosphatase from Saccharomyces cerevisiae reveals the basis for substrate specificity. J Mol Biol 2007;371:1007–21. https://doi.org/10.1016/j.jmb.2007.05.066.

[61] Lonetti A, Szijgyarto Z, Bosch D, Loss O, Azevedo C, Saiardi A. Identification of an evolutionarily conserved family of inorganic polyphosphate endopolyphosphatases. J Biol Chem 2011;286:31966–74. https://doi.org/10.1074/jbc.M111.266320.

[62] Andreeva N, Trilisenko L, Eldarov M, Kulakovskaya T. Polyphosphatase PPN1 of Saccharomyces cerevisiae: switching of exopolyphosphatase and

endopolyphosphatase activities. PLoS One 2015;10:e0119594. https://doi.org/10.1371/journal.pone.0119594.

[63] Ahn K, Kornberg A. Polyphosphate kinase from Escherichia coli. Purification and demonstration of a phosphoenzyme intermediate. J Biol Chem 1990;265:11734–9.

[64] Akiyama M, Crooke E, Kornberg A. The polyphosphate kinase gene of Escherichia coli. Isolation and sequence of the ppk gene and membrane location of the protein. J Biol Chem 1992;267:22556–61.

[65] Akiyama M, Crooke E, Kornberg A. An exopolyphosphatase of Escherichia coli. The enzyme and its ppx gene in a polyphosphate operon. J Biol Chem 1993;268:633–9.

[66] Bayev AY, Angelova PR, Abramov AY. Inorganic polyphosphate is produced and hydrolysed in F0F1-ATP synthase of mammalian mitochondria. Biochem J 2020. https://doi.org/10.1042/BCJ20200042.

[67] Samper-Martin B, Sarrias A, Lazaro B, Perez-Montero M, Rodriguez-Rodriguez R, Ribeiro MPC, et al. Polyphosphate degradation by Nudt3-Zn(2+) mediates oxidative stress response. Cell Rep 2021;37:110004. https://doi.org/10.1016/j.celrep.2021.110004.

[68] Scoma ER, Da Costa RT, Leung HH, Urquiza P, Guitart-Mampel M, Hambardikar V, et al. Human prune regulates the metabolism of mammalian inorganic polyphosphate and bioenergetics. Int J Mol Sci 2023;24:13859.

[69] Tagliafico L, Da Costa RT, Boccia L, Kavehmoghaddam S, Ramirez B, Tokarska-Schlattner M, et al. Short-term starvation activates AMPK and restores mitochondrial inorganic polyphosphate, but fails to reverse associated neuronal senescence. Aging Cell 2024:e14289. https://doi.org/10.1111/acel.14289.

[70] Hambardikar V, Akosah YA, Scoma ER, Guitart-Mampel M, Urquiza P, Da Costa RT, et al. Toolkit for cellular studies of mammalian mitochondrial inorganic polyphosphate. Front Cell Dev Biol 2023;11:1302585. https://doi.org/10.3389/fcell.2023.1302585.

[71] Solesio ME, Prime TA, Logan A, Murphy MP, Del Mar Arroyo-Jimenez M, Jordan J, et al. The mitochondria-targeted anti-oxidant MitoQ reduces aspects of mitochondrial fission in the 6-OHDA cell model of Parkinson's disease. Biochim Biophys Acta 2013;1832:174–82. https://doi.org/10.1016/j.bbadis.2012.07.009.

[72] Solesio ME, Saez-Atienzar S, Jordan J, Galindo MF. 3-Nitropropionic acid induces autophagy by forming mitochondrial permeability transition pores rather than activating the mitochondrial fission pathway. Br J Pharmacol 2013;168:63–75. https://doi.org/10.1111/j.1476-5381.2012.01994.x.

[73] Solesio ME, Peixoto PM, Debure L, Madamba SM, de Leon MJ, Wisniewski T, et al. Carbonic anhydrase inhibition selectively prevents amyloid beta neurovascular mitochondrial toxicity. Aging Cell 2018;17:e12787. https://doi.org/10.1111/acel.12787.

[74] Fossati S, Giannoni P, Solesio ME, Cocklin SL, Cabrera E, Ghiso J, et al. The carbonic anhydrase inhibitor methazolamide prevents amyloid beta-induced mitochondrial dysfunction and caspase activation protecting neuronal and glial cells *in vitro* and in the mouse brain. Neurobiol Dis 2016;86:29–40. https://doi.org/10.1016/j.nbd.2015.11.006.

[75] Gratia S, Kay L, Potenza L, Seffouh A, Novel-Chate V, Schnebelen C, et al. Inhibition of AMPK signalling by doxorubicin: at the crossroads of the cardiac responses to energetic, oxidative, and genotoxic stress. Cardiovasc Res 2012;95:290–9. https://doi.org/cvs134 [pii]10.1093/cvr/cvs134.

[76] Baltanas A, Solesio ME, Zalba G, Galindo MF, Fortuno A, Jordan J. The senescence-accelerated mouse prone-8 (SAM-P8) oxidative stress is associated with upregulation of renal NADPH oxidase system. J Physiol Biochem 2013;69:927–35. https://doi.org/10.1007/s13105-013-0271-6.

[77] Fazzini F, Schopf B, Blatzer M, Coassin S, Hicks AA, Kronenberg F, et al. Plasmid-normalized quantification of relative mitochondrial DNA copy number. Sci Rep 2018;8:15347. https://doi.org/10.1038/s41598-018-33684-5.

[78] Venegas V, Halberg MC. Measurement of mitochondrial DNA copy number. Methods Mol Biol 2012;837:327–35. https://doi.org/10.1007/978-1-61779-504-6_22.

[79] Francis SP, Krey JF, Krystofiak ES, Cui R, Nanda S, Xu W, et al. A short splice form of Xin-actin binding repeat containing 2 (XIRP2) lacking the Xin repeats is required for maintenance of stereocilia morphology and hearing function. J Neurosci 2015;35:1999–2014. https://doi.org/10.1523/JNEUROSCI.3449-14.2015.

[80] Aschar-Sobbi R, Abramov AY, Diao C, Kargacin ME, Kargacin GJ, French RJ, et al. High sensitivity, quantitative measurements of polyphosphate using a new DAPI-based approach. J Fluoresc 2008;18:859–66. https://doi.org/10.1007/s10895-008-0315-4.

[81] Solesio ME, Pavlov EV. Methods of inorganic polyphosphate (PolyP) assay in higher eukaryotic cells. Inorg Polyphosph Eukaryot Cell 2016:81–9.

[82] Seidlmayer LK, Gomez-Garcia MR, Blatter LA, Pavlov E, Dedkova EN. Inorganic polyphosphate is a potent activator of the mitochondrial permeability transition pore in cardiac myocytes. J Gen Physiol 2012;139:321–31. https://doi.org/10.1085/jgp.201210788.

[83] Ning J, Xi G, Clemmons DR. Suppression of AMPK activation via S485 phosphorylation by IGF-I during hyperglycemia is mediated by AKT activation in vascular smooth muscle cells. Endocrinology 2011;152:3143–54. https://doi.org/10.1210/en.2011-0155.

[84] Garcia-Haro L, Garcia-Gimeno MA, Neumann D, Beullens M, Bollen M, Sanz P. The PP1-R6 protein phosphatase holoenzyme is involved in the glucose-induced dephosphorylation and inactivation of AMP-activated protein kinase, a key regulator of insulin secretion, in MIN6 beta cells. Faseb J 2010;24:5080–91. https://doi.org/10.1096/fj.10-166306.

[85] Salminen A, Kaarniranta K, Kauppinen A. Age-related changes in AMPK activation: role for AMPK phosphatases and inhibitory phosphorylation by upstream signaling pathways. Ageing Res Rev 2016;28:15–26. https://doi.org/10.1016/j.arr.2016.04.003.

[86] Yan Y, Krecke KN, Bapat AS, Yang T, Lopresti MW, Mashek DG, et al. Phosphatase PHLPP2 regulates the cellular response to metabolic stress through AMPK. Cell Death Dis 2021;12:904. https://doi.org/10.1038/s41419-021-04196-4.

[87] Giovannini D, Touhami J, Charnet P, Sitbon M, Battini JL. Inorganic phosphate export by the retrovirus receptor XPR1 in metazoans. Cell Rep 2013;3:1866–73. https://doi.org/10.1016/j.celrep.2013.05.035.

[88] Wilson MS, Jessen HJ, Saiardi A. The inositol hexakisphosphate kinases IP6K1 and -2 regulate human cellular phosphate homeostasis, including XPR1-mediated phosphate export. J Biol Chem 2019;294:11597–608. https://doi.org/10.1074/jbc.RA119.007848.

[89] He P, Mann-Collura O, Fling J, Edara N, Hetz R, Razzaque MS. High phosphate actively induces cytotoxicity by rewiring pro-survival and pro-apoptotic signaling networks in HEK293 and HeLa cells. Faseb J 2021;35:e20997. https://doi.org/10.1096/fj.202000799RR.

[90] Zhou X, Yang W, Wang X, Ma T. Isoform-specific effects of neuronal repression of the AMPK catalytic subunit on cognitive function in aged mice. Aging (Albany NY) 2023;15:932–46. https://doi.org/10.18632/aging.204554.

[91] Zimmermann HR, Yang W, Kasica NP, Zhou X, Wang X, Beckelman BC, et al. Brain-specific repression of AMPKalpha1 alleviates pathophysiology in Alzheimer's model mice. J Clin Invest 2020;130:3511–27. https://doi.org/10.1172/JCI133982.

[92] Youle RJ, van der Bliek AM. Mitochondrial fission, fusion, and stress. Science 2012;337:1062–5. https://doi.org/10.1126/science.1219855.

[93] Solesio ME, Saez-Atienzar S, Jordan J, Galindo MF. Characterization of mitophagy in the 6-hydoxydopamine Parkinson's disease model. Toxicol Sci 2012;129:411–20. https://doi.org/10.1093/toxsci/kfs218.

[94] Ge P, Dawson VL, Dawson TM. PINK1 and Parkin mitochondrial quality control: a source of regional vulnerability in Parkinson's disease. Mol Neurodegener 2020;15:20. https://doi.org/10.1186/s13024-020-00367-7.

[95] Ferraz LS, Costa RTD, Costa CAD, Ribeiro CAJ, Arruda DC, Maria-Engler SS, et al. Targeting mitochondria in melanoma: interplay between MAPK signaling pathway and mitochondrial dynamics. Biochem Pharmacol 2020;178:114104. https://doi.org/10.1016/j.bcp.2020.114104.

[96] Toyama EQ, Herzig S, Courchet J, Lewis Jr TL, Loson OC, Hellberg K, et al. Metabolism. AMP-activated protein kinase mediates mitochondrial fission in response to energy stress. Science 2016;351:275—81. https://doi.org/10.1126/science.aab4138.

[97] Li J, Wang Y, Wang Y, Wen X, Ma XN, Chen W, et al. Pharmacological activation of AMPK prevents Drp1-mediated mitochondrial fission and alleviates endoplasmic reticulum stress-associated endothelial dysfunction. J Mol Cell Cardiol 2015;86:62—74. https://doi.org/10.1016/j.yjmcc.2015.07.010.

[98] Gowans GJ, Hardie DG. AMPK: a cellular energy sensor primarily regulated by AMP. Biochem Soc Trans 2014;42:71—5. https://doi.org/10.1042/BST20130244.

[99] Zhao B, Qiang L, Joseph J, Kalyanaraman B, Viollet B, He YY. Mitochondrial dysfunction activates the AMPK signaling and autophagy to promote cell survival. Genes Dis 2016;3:82—7. https://doi.org/10.1016/j.gendis.2015.12.002.

[100] Ebrahimi M, Habernig L, Broeskamp F, Aufschnaiter A, Diessl J, Atienza I, et al. Phosphate restriction promotes longevity via activation of autophagy and the multivesicular body pathway. Cells 2021;10. https://doi.org/10.3390/cells10113161.

[101] Hardie DG. The AMP-activated protein kinase pathway–new players upstream and downstream. J Cell Sci 2004;117:5479—87. https://doi.org/10.1242/jcs.01540.

[102] Steinberg GR, Carling D. AMP-activated protein kinase: the current landscape for drug development. Nat Rev Drug Discov 2019;18:527—51. https://doi.org/10.1038/s41573-019-0019-2.

[103] Block GA, Hulbert-Shearon TE, Levin NW, Port FK. Association of serum phosphorus and calcium x phosphate product with mortality risk in chronic hemodialysis patients: a national study. Am J Kidney Dis 1998;31:607—17. https://doi.org/10.1053/ajkd.1998.v31.pm9531176.

[104] Jin H, Chang SH, Xu CX, Shin JY, Chung YS, Park SJ, et al. High dietary inorganic phosphate affects lung through altering protein translation, cell cycle, and angiogenesis in developing mice. Toxicol Sci 2007;100:215—23. https://doi.org/10.1093/toxsci/kfm202.

[105] Tonelli M, Curhan G, Pfeffer M, Sacks F, Thadhani R, Melamed ML, et al. Relation between alkaline phosphatase, serum phosphate, and all-cause or cardiovascular mortality. Circulation 2009;120:1784—92. https://doi.org/10.1161/CIRCULATIONAHA.109.851873.

[106] Eddington H, Hoefield R, Sinha S, Chrysochou C, Lane B, Foley RN, et al. Serum phosphate and mortality in patients with chronic kidney disease. Clin J Am Soc Nephrol 2010;5:2251—7. https://doi.org/10.2215/CJN.00810110.

[107] Kawai M, Kinoshita S, Ozono K, Michigami T. Inorganic phosphate activates the AKT/mTORC1 pathway and shortens the life span of an alpha-klotho-deficient model. J Am Soc Nephrol 2016;27:2810—24. https://doi.org/10.1681/ASN.2015040446.

[108] Fiermonte G, Palmieri L, Dolce V, Lasorsa FM, Palmieri F, Runswick MJ, et al. The sequence, bacterial expression, and functional reconstitution of the rat mitochondrial dicarboxylate transporter cloned via distant homologs in yeast and Caenorhabditis elegans. J Biol Chem 1998;273:24754—9. https://doi.org/10.1074/jbc.273.38.24754.

[109] Chakraborty A, Koldobskiy MA, Bello NT, Maxwell M, Potter JJ, Juluri KR, et al. Inositol pyrophosphates inhibit Akt signaling, thereby regulating insulin sensitivity and weight gain. Cell 2010;143:897—910. https://doi.org/10.1016/j.cell.2010.11.032.

[110] Mukherjee S, Haubner J, Chakraborty A. Targeting the inositol pyrophosphate biosynthetic enzymes in metabolic diseases. Molecules 2020;25. https://doi.org/10.3390/molecules25061403.

[111] Willows R, Sanders MJ, Xiao B, Patel BR, Martin SR, Read J, et al. Phosphorylation of AMPK by upstream kinases is required for activity in mammalian cells. Biochem J 2017;474:3059—73. https://doi.org/10.1042/BCJ20170458.

[112] Adams J, Chen ZP, Van Denderen BJ, Morton CJ, Parker MW, Witters LA, et al. Intrasteric control of AMPK via the gamma1 subunit AMP allosteric regulatory site. Protein Sci 2004;13:155—65. https://doi.org/10.1110/ps.03340004.

[113] Stokoe D, Stephens LR, Copeland T, Gaffney PR, Reese CB, Painter GF, et al. Dual role of phosphatidylinositol-3,4,5-trisphosphate in the activation of protein kinase B. Science 1997;277:567—70. https://doi.org/10.1126/science.277.5325.567.

[114] Stephens L, Anderson K, Stokoe D, Erdjument-Bromage H, Painter GF, Holmes AB, et al. Protein kinase B kinases that mediate phosphatidylinositol 3,4,5-trisphosphate-dependent activation of protein kinase B. Science 1998;279:710—4. https://doi.org/10.1126/science.279.5351.710.

[115] Sarbassov DD, Guertin DA, Ali SM, Sabatini DM. Phosphorylation and regulation of Akt/PKB by the rictor-mTOR complex. Science 2005;307:1098—101. https://doi.org/10.1126/science.1106148.

[116] Zeng Z, Sarbassov dos D, Samudio IJ, Yee KW, Munsell MF, Ellen Jackson C, et al. Rapamycin derivatives reduce mTORC2 signaling and inhibit AKT activation in AML. Blood 2007;109:3509—12. https://doi.org/10.1182/blood-2006-06-030833.

[117] Kovacic S, Soltys CL, Barr AJ, Shiojima I, Walsh K, Dyck JR. Akt activity negatively regulates phosphorylation of AMP-activated protein kinase in the heart. J Biol Chem 2003;278:39422—7. https://doi.org/10.1074/jbc.M305371200.

[118] Horman S, Vertommen D, Heath R, Neumann D, Mouton V, Woods A, et al. Insulin antagonizes ischemia-induced Thr172 phosphorylation of AMP-activated protein kinase alpha-subunits in heart via hierarchical phosphorylation of Ser485/491. J Biol Chem 2006;281:5335—40. https://doi.org/10.1074/jbc.M506850200.

[119] Chang SH, Yu KN, Lee YS, An GH, Beck Jr GR, Colburn NH, et al. Elevated inorganic phosphate stimulates Akt-ERK1/2-Mnk1 signaling in human lung cells. Am J Respir Cell Mol Biol 2006;35:528—39. https://doi.org/10.1165/rcmb.2005-0477OC.

[120] Chida T, Ando M, Matsuki T, Masu Y, Nagaura Y, Takano-Yamamoto T, et al. N-Myristoylation is essential for protein phosphatases PPM1A and PPM1B to dephosphorylate their physiological substrates in cells. Biochem J 2013;449:741—9. https://doi.org/10.1042/BJ20121201.

[121] Xie L, Rajpurkar A, Quarles E, Taube N, Rai AS, Erba J, et al. Accumulation of nucleolar inorganic polyphosphate is a cellular response to cisplatin-induced apoptosis. Front Oncol 2019;9:1410. https://doi.org/10.3389/fonc.2019.01410.

[122] Garcia D, Shaw RJ. AMPK: mechanisms of cellular energy sensing and restoration of metabolic balance. Mol Cell 2017;66:789—800. https://doi.org/10.1016/j.molcel.2017.05.032.

[123] Filadi R, Pendin D, Pizzo P. Mitofusin 2: from functions to disease. Cell Death Dis 2018;9:330. https://doi.org/10.1038/s41419-017-0023-6.

[124] Kawalec M, Boratynska-Jasinska A, Beresewicz M, Dymkowska D, Zablocki K, Zablocka B. Mitofusin 2 deficiency affects energy metabolism and mitochondrial biogenesis in MEF cells. PLoS One 2015;10:e0134162. https://doi.org/10.1371/journal.pone.0134162.

[125] Biedler JL, Helson L, Spengler BA. Morphology and growth, tumorigenicity, and cytogenetics of human neuroblastoma cells in continuous culture. Cancer Res 1973;33:2643—52.

[126] Patro S, Ratna S, Yamamoto HA, Ebenezer AT, Ferguson DS, Kaur A, et al. ATP synthase and mitochondrial bioenergetics dysfunction in Alzheimer's disease. Int J Mol Sci 2021;22. https://doi.org/10.3390/ijms222011185.

[127] McIntyre B, Solesio ME. Mitochondrial inorganic polyphosphate (polyP): the missing link of mammalian bioenergetics. Neural Regen Res 2021;16:2227–8. https://doi.org/10.4103/1673-5374.310687.

[128] Denaro CA, Haloush YI, Hsiao SY, Orgera JJ, Osorio T, Riggs LM, et al. COVID-19 and neurodegeneration: the mitochondrial connection. Aging Cell 2022;21:e13727. https://doi.org/10.1111/acel.13727.

[129] Luo Y, Ma J, Lu W. The significance of mitochondrial dysfunction in cancer. Int J Mol Sci 2020;21. https://doi.org/10.3390/ijms21165598.

[130] Smith SA, Choi SH, Collins JN, Travers RJ, Cooley BC, Morrissey JH. Inhibition of polyphosphate as a novel strategy for preventing thrombosis and inflammation. Blood 2012;120:5103–10. https://doi.org/10.1182/blood-2012-07-444935.

[131] Labberton L, Kenne E, Long AT, Nickel KF, Di Gennaro A, Rigg RA, et al. Neutralizing blood-borne polyphosphate *in vivo* provides safe thromboprotection. Nat Commun 2016;7:12616. https://doi.org/10.1038/ncomms12616.

[132] Sedzro JC, Smith SA, Scott A, Wang Y, Travers RJ, Hemp R, et al. Anti-polyphosphate monoclonal antibodies derived from autoimmune mice. Res Pract Thromb Haemost 2024;8:102550. https://doi.org/10.1016/j.rpth.2024.102550.

